Remote Sensing of Lake Ice Dynamics in the Lower Kuskokwim River Basin, AK

by

Addison Pletcher

A thesis accepted and approved in partial fulfillment of the

requirements for the degree of

Master of Science

in Geography

Thesis Committee:

Sarah Cooley, Chair

Johnny Ryan, Member

University of Oregon

Spring 2024

THESIS ABSTRACT

Addison Pletcher

Master of Science in Geography

Title: Remote Sensing of Lake Ice Dynamics in the Lower Kuskokwim River Basin, AK

The formation and breakup of lake ice plays a critical role in the hydrology, ecology, and subsistence activities of Arctic regions. However, little research has examined ice phenology in small water bodies and complex deltaic environments, areas that are particularly responsive to climate changes and could provide early indicators of broader environmental shifts. This study uses Sentinel-2 optical imagery to map the timing of lake ice breakup in the Lower Kuskokwim River Basin in southwest Alaska from 2018 to 2023. We detect ice breakup timing in 145,955 lakes, as small as 0.001 km^2, filling a gap in our understanding of finer scale lake ice dynamics. Our results indicate that the average ice breakup date across the study period is May 14, with a standard deviation of 9.6 days. Breakup timing shows significant interannual variability, with the earliest mean breakup occurring on May 6 in 2019 and the latest on May 27 in 2023. The standard deviation in breakup timing also varies, with certain years exhibiting wider variability (e.g., 2019 and 2023) compared to others (e.g., 2018, 2020, 2021, and 2022). Temperature is a primary driver of breakup timing; we identify a statistically significant positive correlation between the date of the 0°C isotherm and breakup timing. Smaller lakes (defined as lakes < 1 km^2) tend to break up earlier than larger lakes (6 days earlier on average), demonstrating a faster thermal response to climatic conditions. We find that the lag interval between the 0°C isotherm and breakup date averages 8.4 days, with smaller lakes exhibiting shorter lag intervals compared to larger lakes. Our analysis of 145,955 lakes over six years demonstrates the utility of Sentinel-2 imagery in accurately detecting ice breakup, typically within 2.8 days of observed dates, despite challenges such as cloud cover, sensor resolution, and temporal gaps. The significant interannual variability, along with notable differences in breakup timing between smaller and larger lakes, underscores the responsiveness of small lakes to temperature fluctuations. These findings emphasize the importance of incorporating high-resolution satellite imagery to capture rapid environmental changes, providing a more nuanced understanding of climatic impacts across diverse lake types.

TABLE OF CONTENTS

LIST OF FIGURES

1 | Introduction

Lakes are a dominant feature of high latitude regions and play a vital role in supporting habitat, subsistence activities, and freshwater resources (Watts et al., 2012; Duguay et al., 2003). These water bodies are seasonally covered by lake ice, which isolates the lake from the atmosphere and thus influences ecology, climate, travel opportunities, and greenhouse gas fluxes (Brown & Dugay, 2010). Lake ice breakup is controlled by a combination of physical characteristics and climatological factors, including but not limited to temperature, precipitation, wind, geographical location, elevation, and morphometry (lake size/depth/shape) (Šmejkalová et al., 2016; Jeffries & Morris, 2007). Of these, temperature has been identified as the primary driver of ice breakup, with fluctuations in air temperature accounting for up to 70% of variation of breakup timing (Šmejkalová et al., 2016; Weyhenmeyer et al., 2004). Like other aspects of the Arctic cryosphere, lake ice is thus highly responsive to fluctuations in climate, particularly air temperature; shifts in its phenology, such as freeze-up and breakup times, are both indexed and established as robust proxies for tracking and evidencing broader climate changes (Schindler et al., 1990; Robertson et al., 1992; Futter, 2003; Weyenmeyer et al., 2004; Assel & Robertson, 1995; Palecki & Barry, 1986; Blenckner et al., 2009; Šmejkalová et al., 2016; Zhang et al., 2021).

As the Arctic warms at rates 2-4 times faster than the rest of the globe (Rantanen et al., 2022), lake ice is thus forming later and breaking up earlier (Šmejkalová et al., 2016; Bring et al., 2016, Dibike et. al, 2011). Earlier ice breakup can impact ecology, seasonal water balance, biogeochemical processes, and greenhouse gas fluxes, as well as socio-economic activities (Brown and Duguay, 2010; Šmejkalová et al., 2016; Zhang et al., 2021). This earlier transition can lead to longer growing seasons for aquatic plants, altering the food web dynamics and potentially affecting water quality, as well as increasing turbulent fluxes (heat, moisture, greenhouse gases) between lakes and the atmosphere (Vihma 2016; Wrona et. al, 2016). Due to the vast spatial extent of Arctic-Boreal lakes and wetlands, it is hypothesized that changes in inland ice phenology could have climatological impacts of a magnitude comparable to those of sea ice loss, although this equivalence has not yet been definitively established (Swart et al., 2009; Prowse, 2011).

Despite the importance of lake ice for ecosystems, local communities, and the broader Arctic hydrologic system, researching lake ice phenology across a range of spatial and temporal scales remains challenging. Many studies rely on in situ data, which is highly valuable for providing consistent, long-term records (Benson, et al., 2000), but is very limited in scope, as very few lakes have long-term in situ observations. On the other hand, models used to observe lake ice phenology have large uncertainties, and many climate models either exclude the influence of lakes entirely or underestimate their effects by including only the largest (Brown & Duguay, 2010). Drivers of local-scale variability and the contribution of lake ice to seasonal hydrology, climatology, and the broader Arctic freshwater cycle thus lack consistent quantification. As such, our understanding remains incomplete, particularly concerning the finer scale drivers, their specific impacts on lake ice breakup, and the subsequent effects on the surrounding environmental systems (Arp et al., 2013; Vihma et al., 2016; Zhang et al., 2021).

Relative to previous approaches, satellite data offers many advantages for researching lake ice processes by providing consistent observations over large areas. In Alaska, for example, previous satellite-based work has uncovered a variety of trends in lake ice phenology. One regional study found that shallow lakes on the North Slope typically experience breakup around July 5th (Surdu et al., 2011). Likewise, an Alaska-wide study identified that 88% of the 4,241 lakes examined showed trends toward earlier breakup (Zhang et. al, 2021). Further observation from a different analysis indicated that the average breakup date for Alaskan lakes was May 27th, with coastal areas showing later dates due to the influence of sea-ice on local climatology (Arp et. al, 2013). However, these previous satellite-derived analyses of lake ice breakup have primarily focused on large (> 1 km^2) lakes despite the fact that small lakes and ponds (<1 km^2) comprise the vast majority (98.7 %) of Alaskan water bodies (Wang et. al, 2016). These small lakes and ponds are particularly sensitive to temperature changes (Surdu et. al, 2011; Zhang & Pavelsky, 2019; Brown & Dugay, 2010; Palecki and Barry, 1986), making them critical yet often overlooked indicators of climate variability. Small lakes also exert outsized contributions to greenhouse gas emissions (Holgerson & Raymond, 2016) and are important for their role in biodiversity support (Smol & Douglas, 2007), and as sensitive indicators of climate change impacts on freshwater ecosystems (Zhang & Pavelsky, 2019). This exclusion of smaller water bodies from previous work means lake ice processes in small, highly connected lakes and complex wetlands remain largely unknown.

In this study, we aim to investigate lake ice dynamics at fine spatiotemporal scales by assessing the use of Sentinel-2 imagery for ice breakup detection. We first build and test a method for lake ice breakup detection in 10 m Sentinel-2 imagery. We then apply this method to track breakup timing in 145,955 lakes in the Kuskokwim Delta region in Southwest Alaska, a complex coastal wetland, over 2018-2023. We use the resulting dataset to examine spatial and interannual variability in breakup patterns and temperature controls in breakup timing. By examining breakup timing in previously unstudied small lakes and ponds, we provide new insight into lake ice dynamics in a complex wetland environment as well as the role of lake size in controlling breakup timing.

1.1 | *Background*

Ice phenology research has long relied upon in situ data to track ice formation and breakup patterns. These ice phenology records can span extremely long time periods, anywhere from 20 to 500 years (Benson, et al., 2000; Sharma et al., 2022). These records are invaluable for historical comparisons and for obtaining detailed, high-quality data which have contributed significantly to our understanding of ice dynamics. For example, detailed records like those from Lake Suwa, Japan, which have been documented since 1443 due to its cultural significance, have helped characterize the changing physical structure of ice over time (Benson, et al., 2000; Zhang, et al., 2023). In situ measurements have also been used to demonstrate ecological effects, such as changes in underwater light penetration affecting aquatic life (Yang et al., 2010). Despite their value, in situ datasets are inherently limited in spatial coverage and cannot fully capture the variability across different regions and smaller water bodies. Even the largest in situ ice phenology datasets, such as the Global Lake and River Ice Phenology (GLRIP) dataset, cover a relatively limited number of water bodies, totaling 865 lakes and rivers worldwide (Benson, et al., 2000), and recent work has created similar datasets for the northern hemisphere, encompassing 78 lakes spanning 578 years (Sharma et al., 2022). While they offer consistent, accurate, and long-temporal-scale data, the scope of in situ observations is inherently limited due to the logistical challenges and costs associated with maintaining widespread and continuous monitoring.

Satellite-derived measurements provide a robust alternative to on the ground observations for detecting ice breakup accurately across thousands of lakes as they can be used to gather data for many water bodies simultaneously and thus expand the scale (and spatial and temporal resolution) of phenology measurements (Zhang, 2021). However, much existing satellite-derived ice phenology work relies on coarse resolution data from MODIS (250 m) or Landsat (30 m), and thus focuses on larger lakes thereby excluding a significant portion of surface water area (Zhang et al., 2021; Arp et al., 2013; Šmejkalová et al, 2016). MODIS, for instance, cannot identify the majority of lakes in northern latitudes (Lehner and Döll, 2004; Downing et al., 2006), resulting in data that may not be representative of landscape-scale ice cover loss (Arp et. al, 2013). This is important, as limited data availability constrains our understanding of the role that increased open water periods in small water bodies play in both local ecosystems and the broader climate system (Vihma et. al, 2016). The use of combined methodologies in ice phenology research is becoming increasingly commonplace, as demonstrated in studies by Zhang & Pavelsky (2019) and Tuttle et al. (2022), which use in situ data to enhance and validate the accuracy and reliability of findings by leveraging the strengths of each. Ice phenology studies often focus solely on regional areas or on specific subsets of lakes, which typically do not overlap, and use different variables for quantifying ice phenology (e.g., total ice cover duration, breakup start, breakup end, date of ice-free water) (Brown and Duguay, 2010). These differences thus pose challenges when examining ice phenology data across sources, as methodological inconsistencies can obscure trends and complicate comparisons (Prowse et al., 2007).

Despite differences in data sources, methodologies and spatial temporal extents, previous studies have consistently found that lake ice cover across northern latitudes is experiencing earlier breakup and later formation, indicating a clear and pressing trend of diminishing ice cover (Bring et al., 2016; Šmejkalová et al., 2016). One of the earliest studies by Magnuson et al. (2000) compiled a large in situ dataset spanning from 1846 to 1995 that revealed a similar pattern of earlier breakup in both rivers and lakes in the northern hemisphere. Complementing these findings, Futter et al. (2003) analyzed volunteer-monitored ice phenology data in south-central Canada, identifying a significant extension of the ice-free season from 1970 to 2003. More recent satellite data studies corroborate these observations; for instance, Surdu et al. (2011) documented that on Alaska's North Slope, ice breakup has been advancing by approximately 0.29 to 0.3 days per year from 1950 to 2011. Šmejkalová's (2016) pan-Arctic projections suggest that spring breakup could occur up to a month earlier in the coming decades. Additionally, Dibike et al. (2011) forecast significant reductions in the thickness (10-15 cm) and duration (15-50 days) of lake ice by mid-century (2040-2079). Zhang et al. (2021) further confirmed these patterns of earlier breakup across Alaska, noting that the impacts of these changes are expected to be more pronounced at more southerly latitudes, in agreement with a review by Bring (2016).

Studies have also identified non-temperature drivers of breakup, primarily related to the physical characteristics and/or location of water bodies. Proximity to river channels and connectivity, as well as the relative closeness of lakes to one another, significantly affect ice timing, with lakes closer to rivers, highly connected, or near each other breaking up sooner (Dolan et al., 2021; Zhang & Pavelsky, 2019). Latitude and elevation have also been identified as influential to ice timing, with higher areas breaking up later than their lower/more southern counterparts (Williams & Stefan, 2006). Morphometry of lakes is yet another influencing factor, playing a role in heat storage, circulation, temperature, and the role of wind (Jeffries and Morris, 2007). Of morphological characteristics, depth has been found to be the most influential factor due to its influence on heating/cooling, though shoreline complexity has also been explored (Korhonen, 2006; Arp et. al, 2013). Despite these many influencing factors, temperature remains at the forefront of ice phenology work due to its dominant effect in influencing breakup.

Changes to breakup timing have profound effects on the local environment. Earlier ice breakup extends the open water season, leading to increased evaporation and heat transfer to the atmosphere, which in turn accelerates heating. This process not only increases evaporative flux, contributing more moisture to and from the atmosphere (Vihma 2016), but also significantly influences the surface energy balance of lakes. The alteration in lake ice phenology has the potential to affect both local and regional climate impacts, necessitating further investigation into the dynamics resulting from a longer open water season (Prowse, 2015; Šmejkalová et al., 2016; Brown and Duguay, 2010). The warming resulting from earlier breakup affects summer water temperatures, altering the water balance and productivity of lakes (Williams et al., 2004; Bengtsson, 2011; Prowse et al., 2011). These changes disrupt seasonal patterns, affecting the surrounding ecology through modifications in thermal stratification, light penetration, nutrient supply, and phytoplankton dynamics (Šmejkalová et al., 2016; Wrona et al., 2016; Zhang et al., 2021). Moreover, as the temperature of lakes increases, so does the emission of greenhouse gases like carbon dioxide, methane, and nitrous oxide, due to enhanced metabolic activity and other processes in the warming waters (Walter et al., 2006; Zhang et al., 2021; Šmejkalová et al., 2016; Cory et al., 2014; Wik et al., 2016). Furthermore, the shift in ice cover seasonality impacts both natural and human systems. Altered ice conditions affect transportation and subsistence activities, as well as commercial and recreational uses of lake and river ice (Instanes et al., 2016; Šmejkalová et al., 2016). This loss of ice poses risks to the safety of local travel during winter and spring and has significant implications for food security (for those relying solely on subsistence harvests) and economic opportunities in remote communities (Herman-Mercer et al., 2011; Herman-Mercer et al., 2019).

Despite widespread findings of earlier ice breakup pointing to the many environmental and socioeconomic impacts across the Arctic, existing research often overlooks lake ice processes in smaller water bodies and complex wetland environments, which are critical for more accurate regional climate and atmospheric flux projections. The global distribution of natural lakes is dominated by those less than 1 km^2 (Downing et al., 2006), a pattern that holds true in Alaska (Wang et al., 2016). These small water bodies influence heat and precipitation fluxes to the atmosphere, potentially altering local and regional climates (Vihma et. al, 2016). They are crucial for the hydrological cycle, affecting groundwater recharge, surface water flow, and evaporation rates, which are vital for understanding regional water balance, especially in areas with high lake density. Additionally, small lakes and wetlands are biodiversity hotspots (Smol & Douglas, 2007); changes to their ice cover can significantly impact aquatic ecosystems, creating inhospitable conditions for some species while potentially allowing new ones to thrive (Vincent et al., 2008). Due to their smaller heat capacity, they are more sensitive to temperature changes and climate effects, making them valuable indicators for early signs of climate change impacts on freshwater ecosystems (Zhang & Pavelsky, 2019). This oversight highlights a crucial gap in our current knowledge and underscores the need for enhanced study of these smaller scales (Šmejkalová et al., 2016). Better understanding lake ice dynamics at fine scales, particularly those previously underrepresented in this type of work, thus fills a key gap in our knowledge of ice phenology.

2 | Study Area

Our study focuses on the Yukon-Kuskokwim River Delta (YKD) in southwest Alaska due to its lake dense nature and proximity to major rivers. This coastal lowland bordering the Bering Sea has been identified as the largest major lake district in Alaska (72,831 km^2) (Arp & Jones, 2009), characterized by an abundance of both small and large lakes. The large majority of the YKD is undeveloped and is a complex wetland delta made possible by low topographical relief and permafrost which restricts drainage (Arp & Jones, 2009; Benke & Cushing, 2011). Sedges, shrubs, willow, and alder are the predominant vegetation in the area, and have been designated as an important area for breeding waterfowl (Benke & Cushing, 2011). The YKD is an unglaciated area and is composed of primarily quaternary marine sedimentary rock, though has areas of volcanic rock (Arp & Jones, 2009). Due to the absence of glaciers during the last glacial maximum, the area acted as a refugium for both terrestrial and aquatic species; it therefore is home to several endemic species (Benke & Cushing, 2011). Permafrost exists within the region sporadically (10-50%), in isolated patches (0-10%), and discontinuously (50-90%) (Obu et al., 2019), though this continues to change with a warming climate. The YKD receives relatively little precipitation compared to the rest of the state of Alaska, historically receiving ~43 centimeters, mainly in the summer and fall seasons between June-October (Arp & Jones, 2009; Benke & Cushing, 2011). Spring temperatures average - 4°C and are generally consistent throughout the area, though summer temperatures are more varied throughout the region with western areas being ~ 4° cooler than their eastern counterparts (Arp & Jones, 2009).

For computational purposes, a smaller area of interest was chosen within the YKD; the Lower Kuskokwim River Basin (LKRB), as defined by the USGS identified 6-digit hydrologic unit (HU) basin (CONCAT 190305) (Seaber et al., 1987). The Kuskokwim River is the dominant feature of this basin and is the second largest and longest river in the state (1,130 km), second only to its northern neighbor, the Yukon River (Benke & Cushing, 2011). The Kuskokwim is sourced from snow and glacier melt, traveling from its source in the Alaska Range as a wide, braided river with many tributaries and a low gradient (Benke & Cushing, 2011). The LKRB is home to several towns including but not limited to Quinhagak, Eek, Tuntutuliak, Kipnuk, Bethel, Aniak, Crooked Creek, Red Devil, among others (Benke & Cushing, 2011); Bethel is the largest populated area in the region with 6,325 people (U.S. Census Bureau, 2020). The majority of land use is used to support subsistence activities, including hunting, fishing, and trapping; pacific salmon and steelhead are the most commercially valuable fish caught in the area (Benke & Cushing, 2011).

The LKRB alone is home to 148,847 lakes and ponds (conservatively), though when including ephemeral water bodies this number would be much higher. Of these, 99.4 % (148,022 lakes) are < 1 km²; these lakes compose 45.84% of the total surface water area of the region. As such, there exists a strong need to study such lakes to better understand ice phenology processes at varied scales (Zhang, 2019), especially important in regions so densely populated with small water bodies like the YKD (Arp & Jones, 2009). Since no comprehensive ice phenology analysis currently exists for this area, this project will fill a data gap in both context-based information for larger lakes, and new information on the area's smallest lakes.

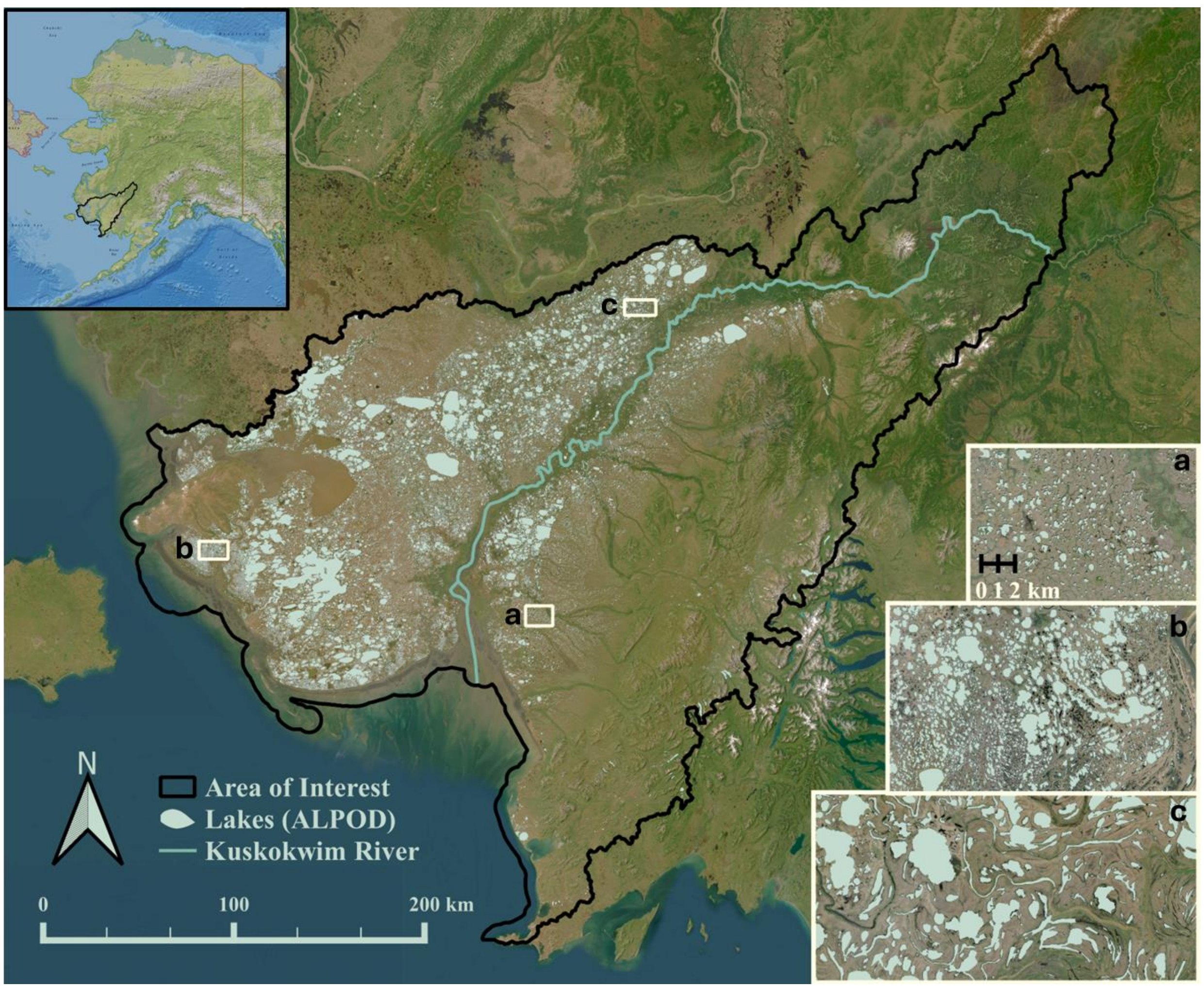

Figure 1: Lower Kuskokwim Basin in southwest Alaska. The Kuskokwim River, shown in teal, flows to the Bering Sea via the Kuskokwim Bay. Inset maps a, b, and c demonstrate the lake dense and complex nature of the region, characterized by 145,955 water bodies.

3 | Methods

3.1 | *Input Datasets*

We chose to test the use of Sentinel-2 imagery for ice breakup detection due to its wide availability and sufficient temporal (<5-day revisit) and spatial (10 m) resolution, as well as the ease of distinguishing between ice and water using optical imagery. Planet imagery offers improved spatial and temporal resolution compared to Sentinel-2; however, Sentinel-2 was favored due to both its free availability and its ease of access in Google Earth Engine. We analyzed data over the spring season (April 1^{st} – June 30^{th}) for 2018 to 2023.

Central to detecting lake ice breakup is an accurate dataset of individual lake objects. Until recently, there were very few high-resolution lake datasets which contain lakes smaller than 1 km^2. Previous ice phenology work has often used the Global Lakes and Wetlands Database (GLWD), which can underrepresent lake prevalence, often accounting for only the largest water bodies. Small lakes and wetlands specifically are often not included in such databases despite being a dominant feature of high latitude regions (Šmejkalová et al., 2016, Bring et. al, 2016). Studies that do have higher resolution masks (ie HydroLAKES) are limited by the resolution of the chosen sensor for ice detection (Zhang et al., 2021). To enable analysis of very small lakes, we used a novel lake mask product, the Alaska Lake & Pond Dataset (ALPOD), that includes all stable lakes within the region (Levenson et. al, in prep), to identify lakes to be used in our analysis. Further details about the method used to produce ALPOD can be found in Levenson et. al, (in prep) but a brief description is provided here. A Sentinel-2-derived product, ALPOD utilizes imagery from 2016-2021 to create an open water occurrence raster representative of maximum lake extent. To do this, a pre trained U-Net classification model was utilized to identify lake extent, followed by manual verification and adaptive NDWI thresholding to identify open water. This method proved extremely accurate with an F1 value of 0.999. Lakes from ALPOD were selected based on a 75% occurrence threshold, meaning they had to be identified as water at least 75% of the time in 2016-2021 to be included in our analysis. Ephemeral lakes as well as those < 0.001 km^2 were excluded to maintain a Minimum Mapping Unit (MMU) of 5x5 pixels, ensuring reliable ice classification as these smallest lakes often contained insufficient pixels to meet this threshold (Lesi, et. al, 2022).

In total, this dataset includes 145,955 water bodies, with a median size of 0.005 km^2 and a mean of 0.0485 km^2, skewed by the presence of a few large lakes. The largest water body in the dataset is 151.98 km^2, though 99.5% of the dataset (145,155 water bodies) is smaller than 1 km^2, accounting for ~45% of the total lake area in our study region.

3.2 | *Detecting Ice Breakup*

We utilized the red band (Band 4: 665nm) of Sentinel-2 (Harmonized Sentinel-2 MSI: Level-1C) for ice classification, as ice is very distinguishable compared to water in red wavelengths and has been used for ice/water detection in previous studies (Pavelsky & Smith, 2004, Zhang et. al, 2019, 2021). Additionally, while the red band can be used to distinguish between ice and water over all lakes, previous work has found performance improves over small/medium lakes (compared to larger lakes), further emphasizing its utility for our purposes (Zhang, 2021). We distinguished between ice and water using a static threshold of 950, which was chosen via manual inspection of reflectance curves from within the region. Images were cloud masked using the maskS2clouds function in Google Earth Engine, which uses the Sentinel-2 QA60 band to create a cloud and cirrus bit mask (10 and 11, respectively) and masks images based on this. All classification and image processing utilized Google Earth Engine's Python API.

We acknowledge that there is uncertainty in this method of ice classification, as thin ice has an altered spectral profile which may lead to missed pixels/ incorrect classification as water, potentially resulting in a negative bias of breakup estimate (Zhang et al., 2021). There are other methods for distinguishing between ice and water that may be more accurate and precise in spectrally identifying ice (mNDWI, NDSI, Sentinel-2 Scene Classification; Barbieux et. al, 2018; Zhang et. al, 2022; Liu et. al, 2021). However, these all rely on bands and/or derived products that only exist at >20m spatial resolution, and given that our analysis focuses on small lakes, we found classifications based on the 10m data were more suitable for our purposes. We also note a dynamic threshold would likely improve the accuracy of the classification on a lake-by-lake basis but found the static threshold to be sufficient for the exploratory nature of this study.

By applying the ALPOD dataset to classified Sentinel-2 images, we produced time series of ice fraction for each of our 145,955 water bodies for each year over April-May. We then filtered the resulting time series by removing 'no data' values as well as observations with more than 10% cloud cover. 'No data' values refer to dates or lakes where the classification did not perform due to a lack of imagery, sensor error, or other external considerations. For computational purposes, ice classification was applied over a tiled scheme and run in batches.

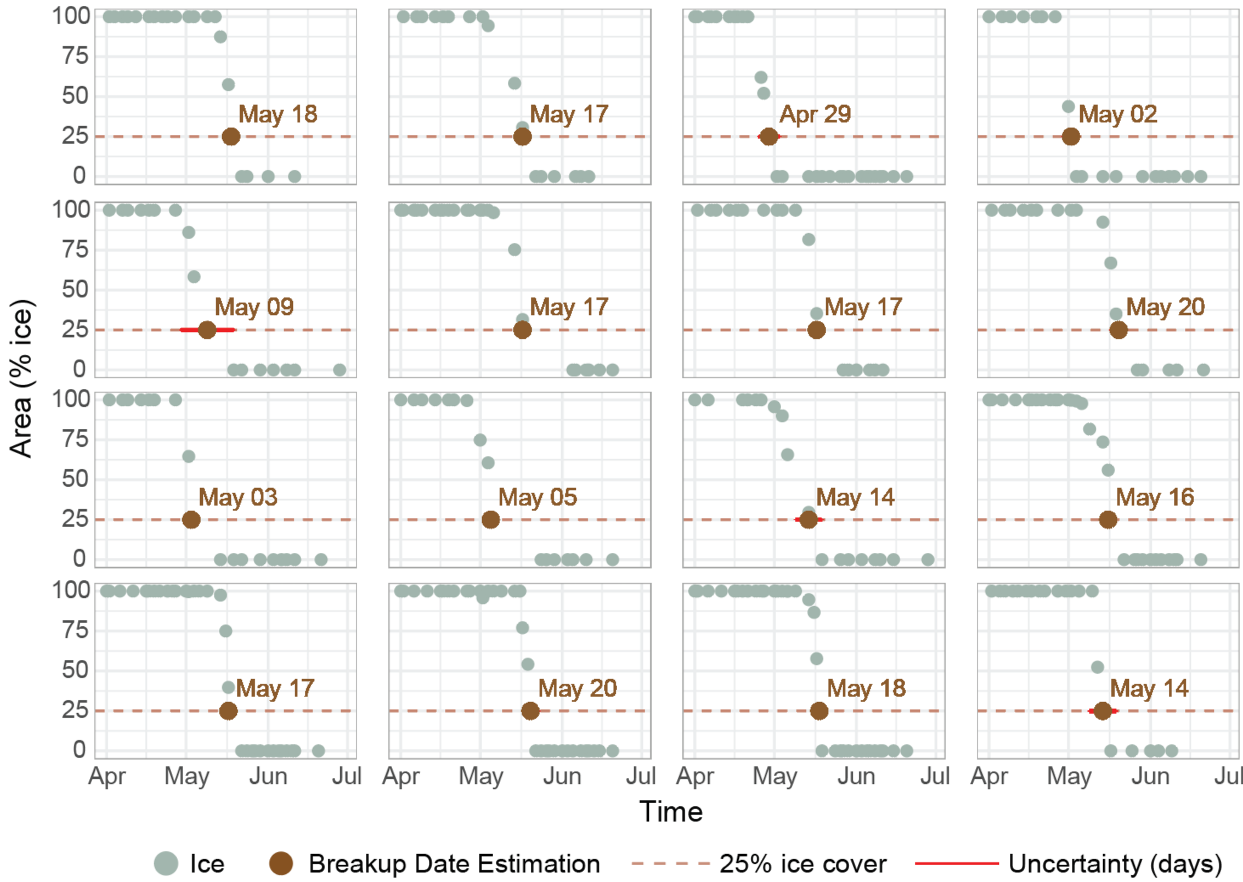

Figure 2: Time series for selected lakes during the 2022 breakup season, generated through classification of Sentinel-2 imagery. Each plot represents a single lake with pale blue dots representing the percentage of ice cover over the breakup period, brown dots indicating our Sentinel-2 derived estimated breakup date using the 25% ice cover threshold (shown as the horizontal dashed line). Uncertainty, defined as the number of days between the observations bounding breakup date, is shown with a horizontal red line.

Thresholds for identifying breakup vary by study, ranging from ice coverage of 10-20% (Arp et al., 2013; Zhang et al. 2019, 2021). In this study, we define ice breakup using an ice fraction of 25% or less (i.e. at least 75% open water); this decision was driven by the large number of small lakes analyzed. Small lakes have a higher perimeter-to-area ratio, making them more susceptible to localized variations at their edges. Using a higher threshold helps mitigate the influence of these edge effects, as it ensures that the breakup detection is not prematurely triggered by minor edge melt and/or mixed-pixel contamination, thus providing a more accurate and representative measure of ice breakup. Due to cloud cover and the approximately 2-3 day temporal resolution of Sentinel-2 (at a latitude of ~60° N), there were often gaps in observations that required estimating the true breakup date. Linear interpolation between the two closest valid (cloud-free) observations was used to determine the breakup date, similar to the methodology of Zhang (2021). The uncertainty of the breakup date was defined as the number of days between these observations (Cooley et al., 2020).

3.3 | *QA/QC of red band ice classification*

Satellite-derived ice breakup timing is best validated through local in situ observations; however, such data are scarce for this region. The absence of ground-level data necessitated the validation of lake ice breakup via manual analysis of satellite imagery. By employing a combination of PlanetScope, Sentinel-2, and Landsat imagery, we achieved the desired temporal resolution for this analysis. To verify the accuracy of our breakup date estimations, we manually determined the breakup timing for selected lakes using this integrated satellite imagery approach. 175 lakes were randomly selected using a stratified sampling method to ensure variance of geographic location and lake size. As there are many more small than large lakes, we wanted our sampling method to be representative of each group. Lakes were binned by quintiles into five groups by size, and the number of lakes chosen for QA were thus proportionate to the prevalence of said group in the dataset (all groups being required to have at least one lake). To account for a varied geographic spread of samples, the ROI was split into quadrants, lakes being sampled from each. We then compared manually detected breakup dates with estimated breakup dates, computing the difference in estimations in days. We find the average performance of our Sentinel-2 derived breakup date estimation to be within 2.8 days of the manually detected breakup date. This level of precision indicates that while the automated method provides a reliable estimate, there is still a minor margin of error that can be attributed to factors such as cloud cover, sensor resolution, and temporal gaps between satellite overpasses, highlighting the need for continued refinement.

3.4 | *Temperature*

We use the ERA-5 Land reanalysis product (Muñoz-Sabater, 2019) for temperature data (2 meters) due to its comprehensive spatial and temporal coverage, which ensures a representative and accurate assessment of temperature variations across our study area. While local in situ temperature gauges provide valuable point measurements, they can be influenced by microclimatic conditions that are not suitable for extrapolation across larger regions. This high-resolution data is validated and widely used in climate and environmental research (Webb et al., 2022; Cooley & Ryan, 2024), and has been shown to perform well in high latitude environments (Graham et al, 2019). Temperature data was acquired via the Copernicus ERA5 Daily Aggregate dataset, accessed via Google Earth Engine (2018-2020) and Copernicus' Daily Statistics Calculator (2021-2023); due to internal site maintenance, GEE had limited records resulting in the necessary use of CDS's aggregate product. Temperature data was then intersected with each lake's geographic location.

We choose to focus on the 0° Celsius isotherm date for assessing temperature controls on breakup timing, as previous work has shown it is useful in predicting ice breakup at the regional scale (Arp, 2013). The 0°C isotherm is defined as the day when daily mean air temperature crosses the 0°C threshold when smoothed over a 31-day period (Šmejkalová et al., 2016). In other words, it represents the first day when the temperature over the 31 days prior has averaged 0°C or above. This metric has a proven relationship to ice phenology, with the 0°C isotherm typically preceding breakup by a few days up to a month (Brown et. al, 2006).

To quantify the relationship between temperature and breakup, we difference the date of breakup from that of the 0°C isotherm to derive the approximate period between which melting begins and ends, defined as the lag interval. To assess the predictive power of lag intervals from the 0°C isotherm, we average the lag for each lake over 2018-2023, then add the average lag to the date of the 0°C isotherm to produce a temperature lag-estimated breakup date. We then compare lag estimated breakup to Sentinel-2 estimated breakup.

3.5 | *Lake Size*

A key question motivating this analysis is the relationship between lake size and breakup timing. To test this, we analyzed the breakup results by binning data into two groups, lakes larger and smaller than 1 km^2. We choose this particular size grouping as most prior research has been limited to lakes > 1 km^2. We then perform summary statistics and visualizations to examine breakup timing in each size group. Additionally, we investigated the relationship between the lake size and lag time, using the same grouping method to understand if and how the lag time varies with lake size.

4 | Results

4.1 | *Lake Breakup Results*

Over our 145,955 lakes over 2018-2023, we find that on average breakup occurs on May 14, with an average standard deviation of 9.6 days over the 6-year period. The mean (median) of yearly breakup varies ranges from May 6 (May 3) in 2019 to May 27 (May 27) in 2023. The proximity of mean/median values within each year suggests a minimal skew in the data. The standard deviation in breakup timing also varies from year to year, with some years (2019, 2023) having wider variability with a standard deviation of ~12 days, whereas others (2018, 2020, 2021, and 2022) demonstrate more concentrated distributions with standard deviations ranging between 7-9 days. Interquartile ranges (IQR) for lake ice breakup dates exhibit variability across the years studied, with a maximum range of 18 days in 2023 compared to narrower ranges of 9 days in both 2020 and 2021. The first (Q1) and third (Q3) quartiles of breakup dates also show notable fluctuations, with Q1 ranging from April 29th in 2019 to May 18th in 2023, and Q3 extending from May 12th in 2019 to June 5th in 2023. Notably, the year 2023 observed earlier

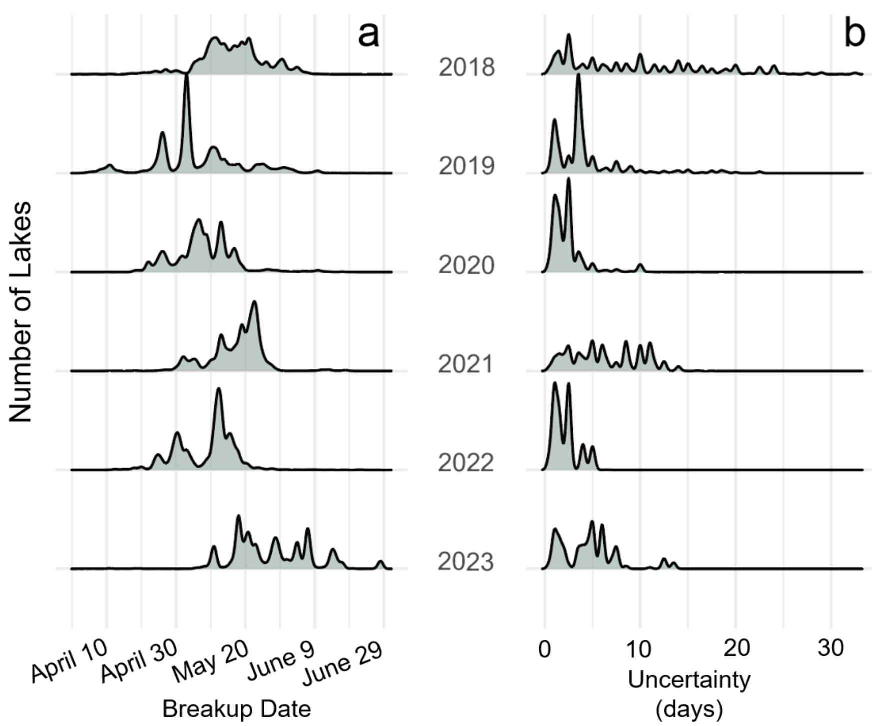

Figure 3: Distribution of breakup date and associated uncertainty by year

breakup dates compared to 2019, as reflected in the broader span between the 25th and 75th percentiles (Figure 3a).

The uncertainty in breakup dates (defined as the number of days between valid observations, i.e. the period over which linear interpolation occurs) averages ± 4.4 days but exhibits significant interannual variability, as shown by the broad range of maximum uncertainty values observed across different years (Figure 3b). The lowest mean uncertainties occur in 2020 and 2022 (± 2 days), while 2018 and 2021 have the highest mean at ± 9.3 and 6.4 days. A similar pattern follows for the IQR, with the lowest spreads in 2019, 2020, and 2022 (± 1.5-2.5 days) and the highest in 2021 and 2018 (± 6.5-11.5 days). While most lakes each year exhibit low uncertainty in breakup dates, all years (except 2022) also experience high levels of uncertainty exceeding ± 5 days. That said, the proportion of lakes experiencing such high levels of uncertainty varies significantly by year. For instance, in 2022, nearly all lakes (99.8%) had uncertainty within ±5 days, indicating a highly precise year for breakup date estimations. Conversely, in 2021, less than half of the lakes (46.0%) showed this level of certainty, reflecting greater variability in breakup timing predictions within that year. The percentages of lakes with uncertainties within ±2 days also reveal interesting patterns; 2022 again shows the highest precision with 52.6% of lakes falling within this narrower uncertainty range, highlighting its consistency in predictions. On the other hand, 2021 displayed much lower precision, with only

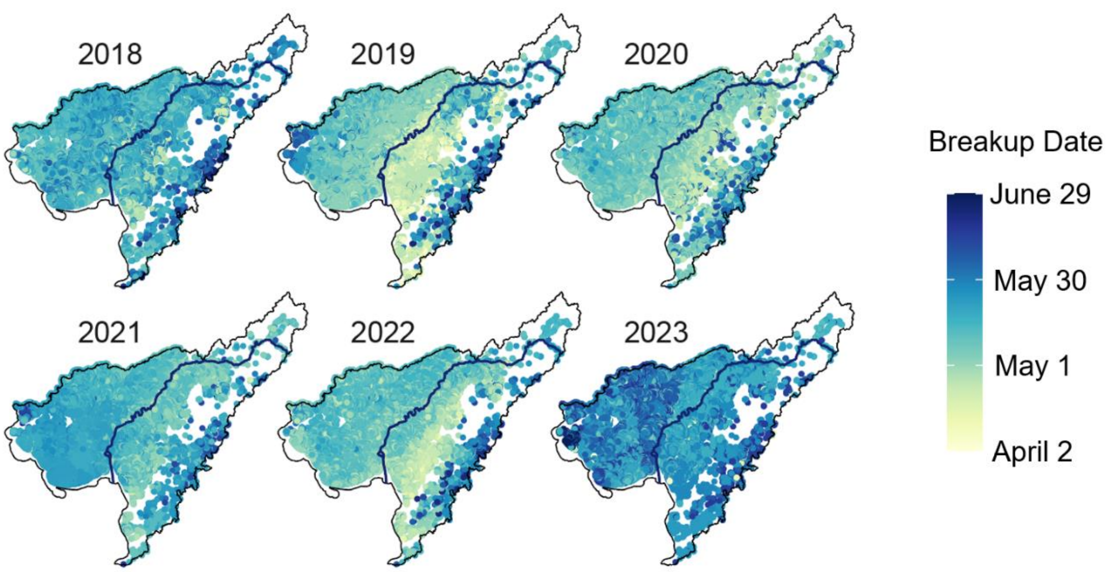

Figure 4: Estimated breakup date maps. Each dot represents an individual lake, and the line down the middle shows the location of the Kuskokwim River main channel. Earlier breakup is shown in yellow and later breakup in blue.

14.6% of lakes having breakup uncertainties within ±2 days, underscoring a year of considerable unpredictability in ice breakup timing.

Spatial patterns in breakup timing generally reveal both interannual and spatial variability (Figure 4). In general, the areas closest to the southeast of the Kuskokwim River (directly to the east of the river in Fig. 4) break up first (~ May 13), whereas the higher elevation lakes to the southeast of our study area break up last (~ June 19). We also see later breakup dates in highly localized fashion toward the most western region near the ocean (end of May, start of June). Not all years follow these patterns exactly, indicating that while local physiography certainly plays a role in controlling breakup, interannual variability in climate and other conditions is also important.

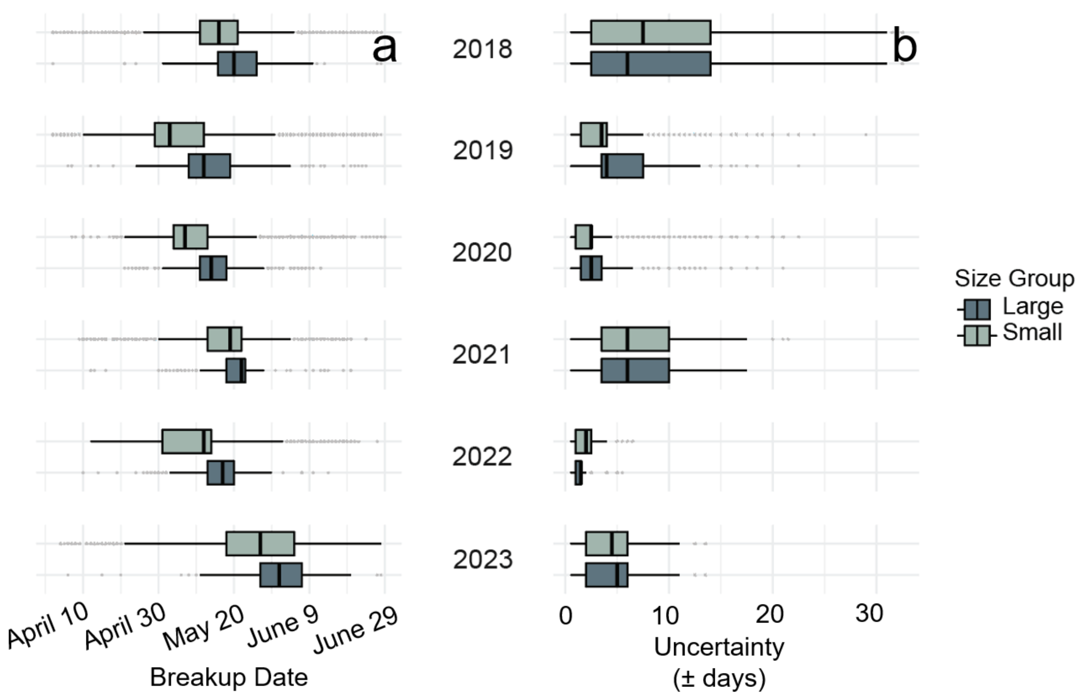

Figure 5: Yearly breakup date and associated uncertainty by size group.

We find, on average, breakup consistently occurs earlier in smaller lakes, with mean breakup for lakes < 1 km^2 occurring on average 6 days earlier than larger lakes (ranging from 3 days in 2021 to 9 days in 2022) (Figure 5). This pattern is consistent across all years and demonstrates that smaller lakes respond more rapidly to spring warming than larger lakes. The IQR for each year shows considerable variability and is more sensitive to interannual changes than to differences in lake size. For example, the IQR varies significantly between years, with an average difference of 7.5 days (ranging from 7 days in 2021 to 14.5 days in 2023). In contrast, the IQR difference between lake sizes is narrower, with an average difference of 3.5 days (8.5 days for large lakes and 12 days for small lakes). This wide interannual range of possible breakup dates (7-14.5 days), observed across all years and lake sizes, underscores that while lake size does influence the timing of breakup, it is just one of many factors. The persistent breadth of this range highlights that while size influences the timing of breakup, other factors such as local climatic conditions and specific lake characteristics also play significant roles. Uncertainty varies little by lake size and is similarly more tied to interannual variability. We observe this through the similarity of means within years; each yearly mean varies at most by 2 days between small vs. large lakes, while interannually means vary by an average of ~7 days. This suggests that the primary drivers of uncertainty in breakup dates are yearly climatic conditions rather than lake size. Overall, while smaller lakes tend to break up earlier, the variability and uncertainty in breakup dates are more strongly controlled by interannual climatic variability than by lake size alone.

4.2 | *Temperature Analysis*

Across all years, the average date of the 0°C isotherm is May 5 (Figure 6). Interestingly, we find a general trend with an increasing 0°C isotherm date over 2018-2023, with 2023's average crossing date (May 17) occurring 16 days later than that of 2018 (May 1). The IQR is small for most years (1-5 days), with the exception of 2019 (20 days), indicating consistent crossing dates among most lakes within years. 2019's wide variability range is reflected in Figure 6 where we observe a higher spread of isotherm dates compared to other years. The yearly mean for isotherm date generally falls between April 30 and May 7, though 2023 is notably colder with a mean isotherm date of May 17. Spatially, isotherm dates follow similar patterns through time, with the earliest dates occurring in the central area near the Kuskokwim River and the latest dates occurring at the northwestern and southeastern areas of the study area.

Some years show generally consistent isotherm dates throughout the entire study area (2021, 2023), while others are more variable (2018, 2020, 2022 and especially 2019).

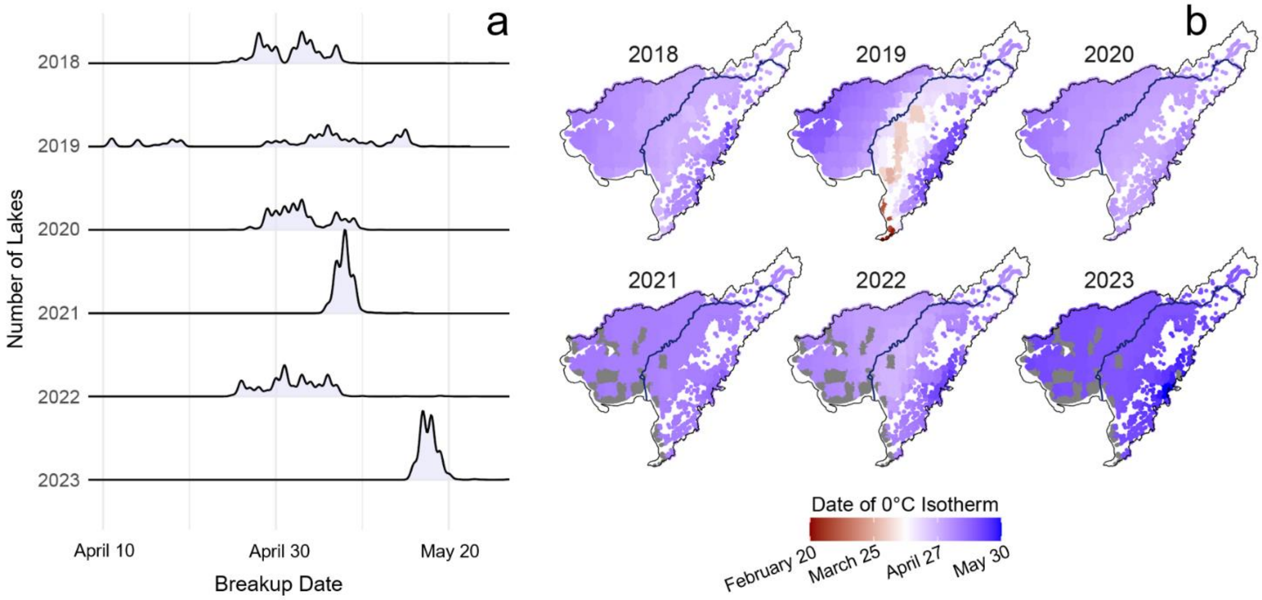

Figure 6: Distributions of yearly temperature patterns from 2018-2023. a) Yearly distribution of the 0°C isotherm dates b) Yearly maps of temperature patterns, visualized as the date of the 0°C isotherm over each lake. Areas in grey indicate no available data.

4.2.1 | Relationship between Temperature and Breakup

To investigate if warmer years break up earlier and/or faster than colder years, we examine the relationship between the timing of the 0°C isotherm and breakup (Figure 7). Across all years, there exists a positive correlation between isotherm date and breakup timing ($R^2 = 0.31$, $p < 0.0001$), suggesting that earlier warming leads to earlier breakup, and vice versa. While the relationship between isotherm date and breakup timing is positive and statistically significant within each year individually as well, there is some notable interannual variability in the strength of this correlation. For example, in 2018 the correlation is weaker ($R^2 = 0.0004$, $P < 0.0001$), perhaps due to the increased uncertainty in breakup timing this year. The statistically significant but low R^2 values indicate that while temperature does have a significant role in breakup timing, there are other factors influencing the breakup date (wind, connectivity, lake size, as well as breakup detection uncertainty). These findings highlight the complexity of lake ice breakup prediction and underscore the need for a robust approach to accurately forecast these events.

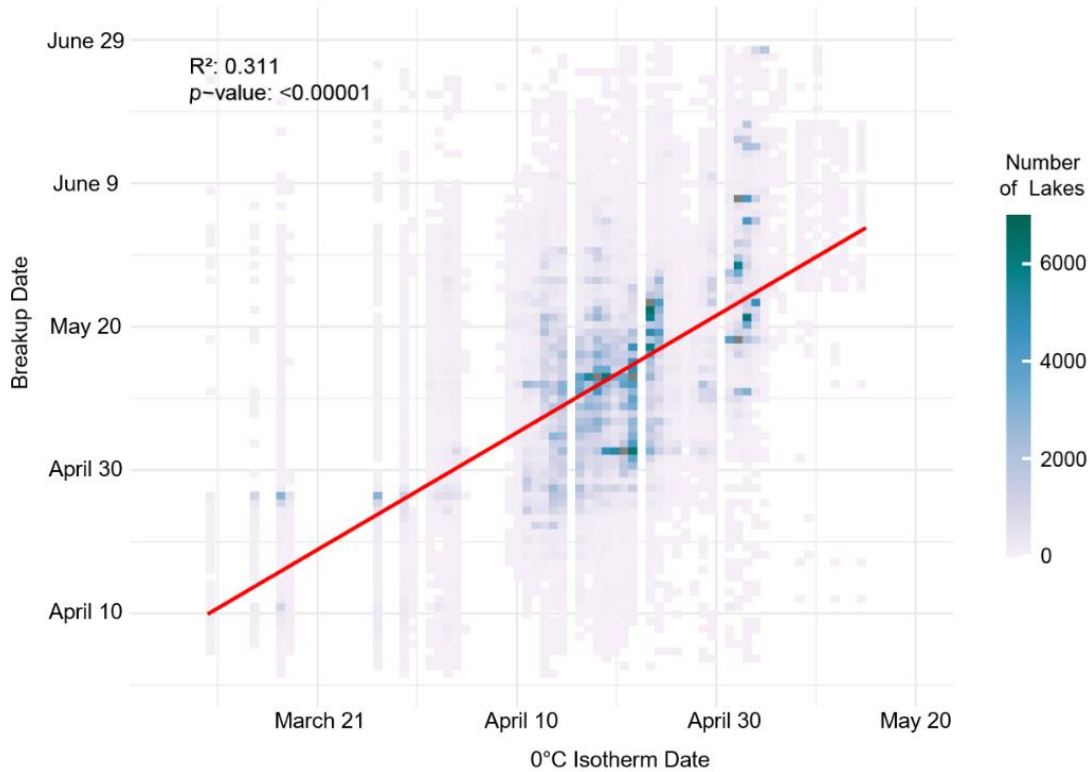

Figure 7: Relationship between 0°C isotherm date and breakup date for all years; Red line indicates linear regression.

4.2.2 | Yearly Lag Interval

The mean lag interval between the 0°C isotherm and breakup date across all lakes and all years is 8.4 days, ranging from 5 days in 2020 to 14 days in 2018 (Figure 8(a)). In other words, on average breakup occurs 8.4 days after the date of the 0°C isotherm. In all years some lakes (18.7% on average) break up before the 0°C isotherm; however, the vast majority of lakes breakup after the date, suggesting it may have some predictive capacity. The wide IQRs in lag interval (15-16 days) in 2019 and 2023 indicates the widest variability in lag interval, pointing to a range of conditions among lakes during that year. In contrast, 2020-2021 are characterized by more consistent lag intervals (IQRs of 9 and 8), while 2018 and 2022 fall in the middle with IQRs of 13 and 11.

Spatially, lag intervals display some regional patterns, though interannual variability appears to be generally larger than the effect of geographic location (Figure 8b). Variability within years is likely influenced by local climatic conditions. For example, in 2018, the maps predominantly show longer lag intervals, while 2019 exhibits a mix of longer and shorter lag intervals, suggesting more variability in how lakes responded to temperature changes that year.

Notably, the years 2019 and 2022 display higher variability in lag intervals, which might be indicative of specific climatic events or anomalies affecting those years.

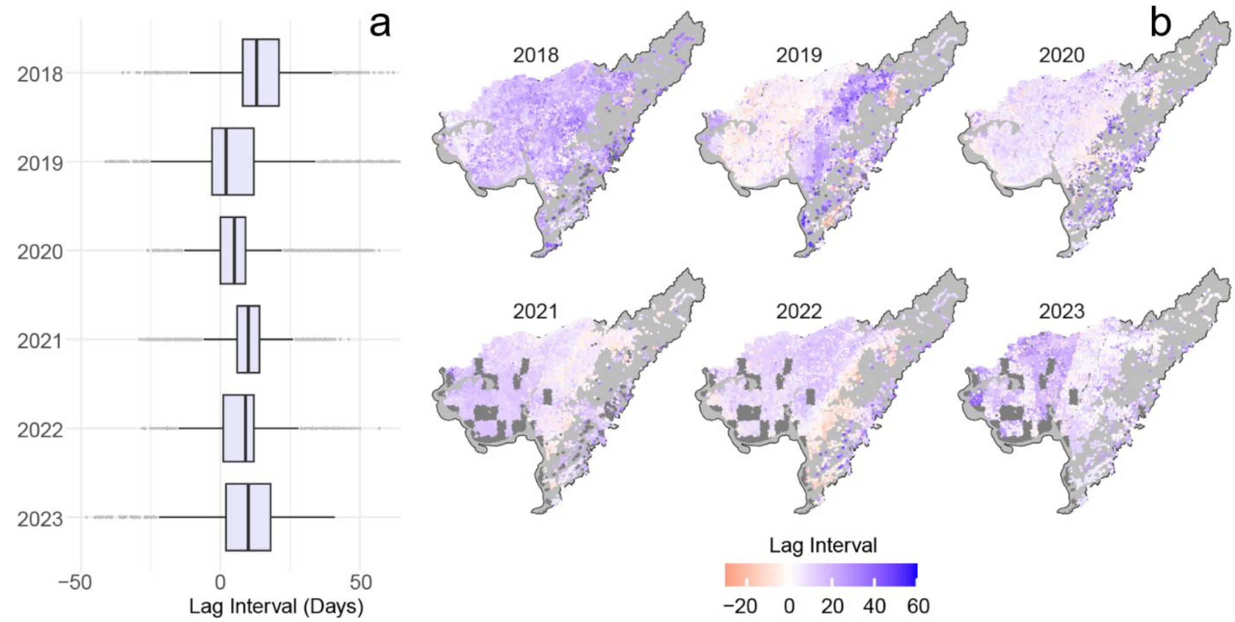

Figure 8: Distribution of yearly lag interval (in days) from 2018-2023.

When examining lag interval by lake size, we find the mean lag interval for small versus large lakes to be 8.3 and 14.1 days, respectively. We observe small lakes to consistently have a shorter mean lag interval than larger lakes by an average of 5.8 days, ranging from 3.6 days earlier in 2021 to 7.9 days in 2022 (Figure 9). We note this is approximately the same as the difference in breakup timing as there is not a statistically significant difference in 0°C isotherm date between small vs. large lakes. This consistent pattern again implies the faster thermal response of smaller lakes to climatic conditions compared to larger lakes. Furthermore, the IQR for lag interval in small lakes, averaging 12 days, is wider than that of large lakes, which averages 9.6 days. Despite these differences in lag variance by size, there is still considerable variability in lag interval across all lakes, suggesting that factors such as localized conditions also play a crucial role in influencing breakup dynamics.

Interestingly, when investigating the relationship between temperature and lag interval, we observe a general pattern where later 0°C isotherm dates are associated with shorter lag intervals towards breakup timing ($R^2 = 0.02$, p value = 0.0) (Figure 11). In other words, colder years breakup faster after the 0°C isotherm than warmer years. This negative correlation between

0°C isotherm date and lag interval is evident in both the overall dataset and when comparing warm and cold years separately.

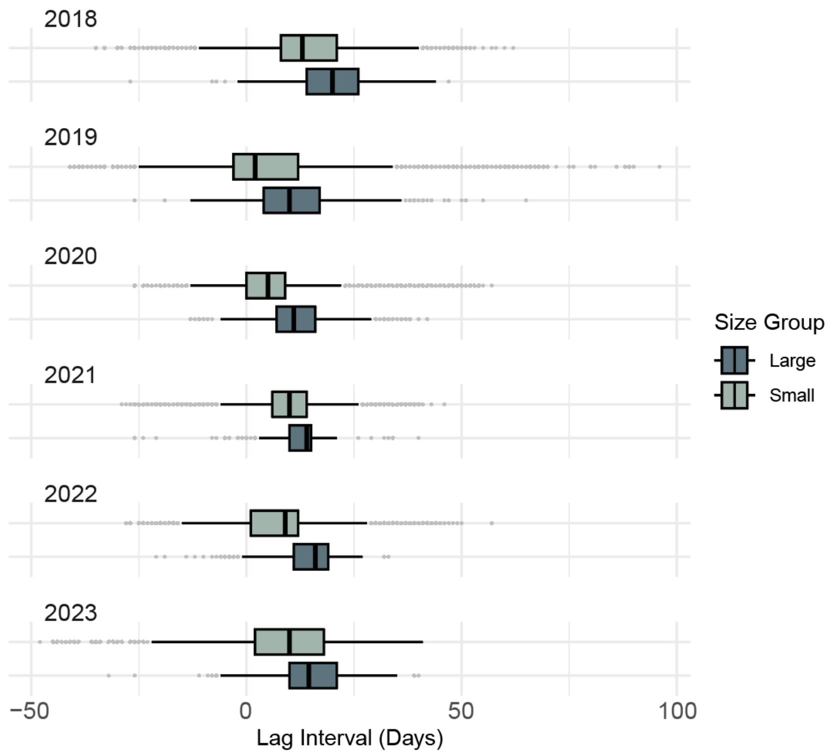

Figure 9: Yearly lag interval by size group, computed as the difference between the date of the 0°C isotherm and breakup

4.2.3 | Lag Interval as Breakup Predictor

To investigate the efficacy of using average lag time to predict breakup dates, we compared lag-estimated breakup dates to previously estimated breakup dates from Sentinel-2 (S2) imagery (Figure 11a). Our analysis reveals a general pattern where the lag prediction method tends to overestimate breakup timing early in the season (March 31-April 20) and underestimate it later in the season (May 30-June 29). There is strong agreement between both methods during the middle of the season (April 20-May 30), reflected by the lowest mean absolute error (5-10 days), where the highest density of lakes aligns most closely with the 1:1 line. However, this alignment could be due to the higher data availability in this period rather than improved accuracy, as most data points fall between April 30-May 20.

When examining the predictive power of the lag time breakup estimation across different lake sizes, we found that both size groups performed similarly. The mean absolute error for smaller lakes is approximately one day longer than that for larger lakes (6.8 vs. 5.7), suggesting that larger lakes are estimated slightly more accurately. Additionally, smaller lakes exhibit higher variability in their error compared to larger lakes, with standard deviations of 5.7 and 4.7, respectively.

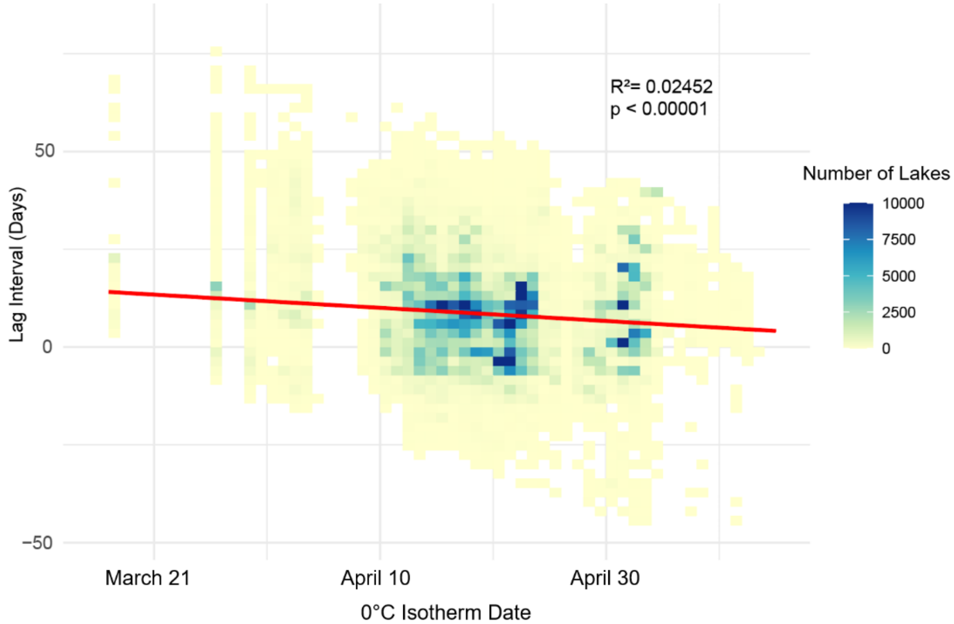

Figure 10: Relationship between temperature isotherm date and lag interval, showing a general trend of shorter lag interval with later isotherm date occurrence. The downward sloping linear regression is shown in red.

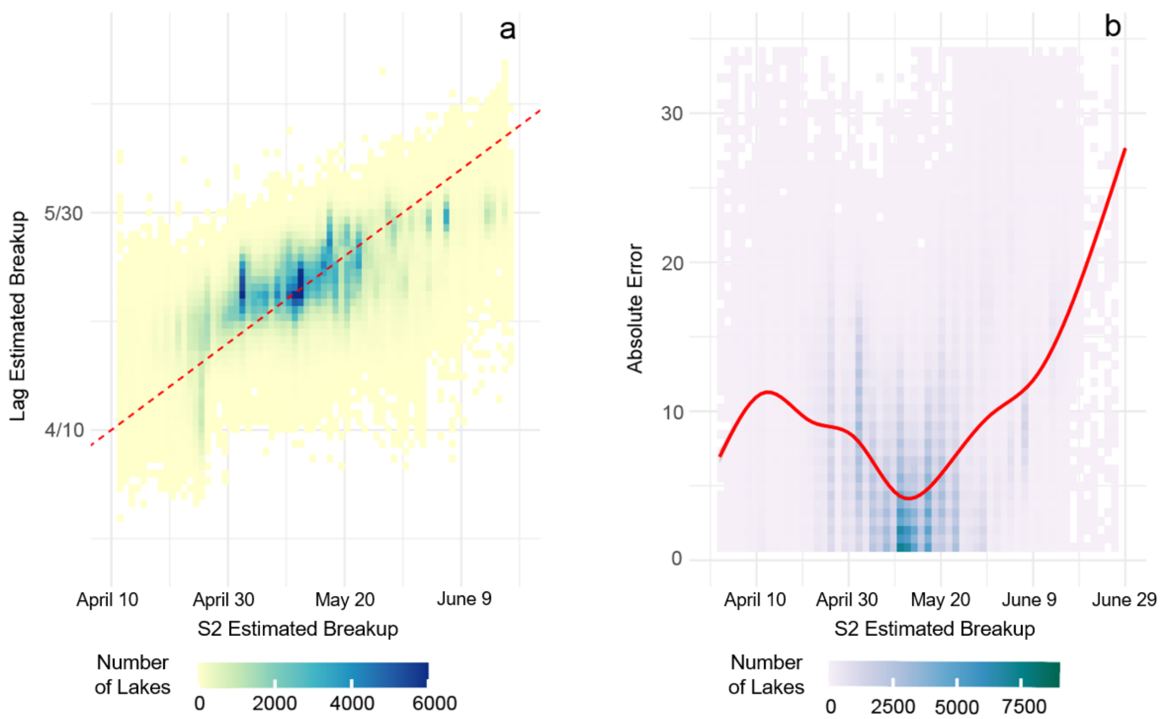

Figure 11: (a) Efficacy of lag as a breakup estimator for all years combined. Red dashed line indicates a 1:1 relationship; (b) Error over time. Solid red line indicates a smoothed trend line (fitted with a generalized additive model).

5 | Discussion

Our analysis of 145,955 lakes over six years suggests that Sentinel-2 imagery can be used for accurately detecting breakup timing in very small water bodies with an uncertainty due to cloud cover of ± 4.4 days (ranging from ± 2 days in 2020 and 2022 to ± 9.3 days in 2018) and an error (compared to manually detected breakup date) of 2.8 days. Cloud cover was the strongest contributor to uncertainty and error, particularly during the breakup season and in SW Alaska, where clouds are especially persistent during the shoulder seasons (Zhang 2021). Over the region, cloud cover reduced data availability by approximately 50%, leading to significant data gaps and impacting the accuracy of analyses. Consequently, there remains uncertainty due to estimation during cloudy periods. The interannual variability of uncertainty emphasizes the need for continued refinement of this method. However, the generally small uncertainty windows and our ability to accurately detect breakup in very small water bodies suggests that despite issues with cloud cover, Sentinel-2 can be used to advance understanding of ice phenology at a fine - scale. Overall, the application of Sentinel-2 for tracking lake ice breakup provides valuable and large-scale information on the areas smallest water bodies; the level of precision observed underscores the utility of Sentinel-2 as a reliable tool for monitoring ice breakup. Our large dataset of ice breakup timing derived from Sentinel-2, novel in its scale which includes many thousands of small lakes, thus enables novel insights into lake ice processes.

5.1 | *Interannual Variability and Spatial Patterns*

Our results indicate that interannual variability generally exceeds spatial variability in ice breakup timing in the Lower Kuskokwim River Basin. This result is perhaps unsurprising given the comparatively small size (88,811 km^2) and small elevation range (0 – 4815 m) of our study region. However, it does imply that local physiography and geomorphological features such as connectivity and proximity to the river may not be as important as climatic processes and therefore that breakup timing observed in a handful of lakes is likely representative of overall breakup patterns within that region. Our finding of comparatively minimal spatial variability in breakup timing across a large number of lakes (145,995) thus yields confidence to analyses/conclusions of large-scale trends in lake ice breakup based on in situ records as it suggests that individual lake time series are likely to be broadly representative of regional patterns.

5.2 | *Temperature Influence on Breakup and Lag Interval*

We found a statistically significant, positive relationship between air temperature and breakup timing, with warmer years generally experiencing earlier breakup. This relationship is supported by previous studies that point to air temperature as a primary driver of lake ice phenology (e.g., Schindler et al., 1990; Robertson et al., 1992; Futter, 2003). However, the variability in the strength of this correlation as well as in lag time between the start of thaw and ice breakup suggests that other factors, such as local climatic conditions and specific lake characteristics, likely also contribute to breakup patterns.

The lag interval method (i.e. using a lake's average lag interval as a breakup predictor) demonstrates moderate effectiveness as a predictive tool for breakup timing, achieving an average accuracy of ± 6.8 days. However, its performance varies throughout the breakup season; it overestimates breakup dates early in the season and underestimates them later. This pattern could be influenced by several factors, including the physical properties of ice and seasonal climatic variations, which may affect the ice melting processes differently at different times of the year. The observed discrepancies in early and late-season predictions point to potential areas for refining the lag interval method. Interestingly, the size of the lakes does not significantly impact the predictive success of the lag interval method. This suggests that the method's core parameters may be robust across different scales, but also indicates that lake-specific characteristics such as depth and water composition, which are not necessarily size-dependent, could be affecting the breakup dynamics.

Accurate predictions of ice breakup have the potential to enhance public safety and the efficiency of subsistence practices. With timely information and/or advance knowledge of local ice conditions, communities can better plan and execute essential activities such as fishing and hunting, while minimizing the risk of accidents associated with unexpected ice loss (Herman-Mercer et al.). Future research should focus on integrating more comprehensive environmental variables to better represent these the complex interactions at play in ice breakup more effectively. Additionally, extending the analysis to include a broader range of geographical locations could help verify the method's applicability and identify specific conditions under which it performs best.

Notably, we find a negative correlation between temperature and lag interval, indicating that colder years break up sooner after the 0°C isotherm date than in warmer years. We hypothesize that the differences in breakup timing across years can be largely attributed to variations in solar insolation, which is influenced by seasonal changes in the sun angle. In warmer years, ice begins to thaw earlier in the season when solar insolation is lower. Due to this lower sun angle, sunlight is less direct and is spread over a larger area, diminishing the amount of solar energy available to thaw ice. Conversely, in colder years, thaw typically initiates closer to the summer solstice (~June 21), benefiting from a higher sun angle and, consequently, more direct solar insolation. This not only increases the rate of thaw but also amplifies the ice-albedo feedback (Ingram et al., 1989; Austin et al., 2007; Lang et. al, 2017), leading to more rapid changes in ice conditions and hence shorter lag intervals. The ice-albedo feedback is crucial, as thawing ice exposes darker surfaces that absorb more sunlight, accelerating local temperature increases and further ice loss. This effect is especially pronounced in colder years when breakup starts later but occurs under more direct sunlight, intensifying the feedback loop. This relationship between temperature and lag interval has important implications for lake ice breakup in a warming climate that warrant additional investigation. While we expect breakup to occur earlier as the climate continues to warm, some of this warming effect may be mitigated by the weaker solar insolation earlier in the spring, suggesting both a potentially longer melt season and a potential non-linearity in future changes in breakup timing.

5.3 | *Influence of Lake Size*

Our novel analysis of breakup timing in thousands of lakes as small as 0.001 km^2 reveals that smaller lakes tend to break up sooner than larger lakes consistently across all years. Smaller lakes also exhibit shorter lag intervals, indicating a faster thermal response to climatic conditions. This is likely due to the smaller heat content required to break up ice in smaller lakes as well as increased warming from the surrounding land. While previous studies have not identified a strong relationship between lake size and breakup timing (Zhang et. al, 2021), this work did not include lakes smaller than 1 km^2, the central focus of this study. Our results support the hypothesis that small lakes will be more responsive to temperature changes under climate change conditions (Vihma et al., 2016). Additionally, the presence of bedfast ice in small lakes, where ice is in contact with the lakebed, could contribute to earlier breakup dates compared to floating ice within the same region; previous studies have shown that bedfast ice can break up approximately 15 days earlier than floating ice (Arp et al.).

5.4 | *Anomalous Year: 2019*

Though our record only spans six years, 2019 had notably anomalous ice breakup patterns. Breakup occurred 8 days earlier in 2019 than the 2018-2023 mean (Figure 3), and the 0°C isotherm also occurred earlier. While the mean isotherm date in 2019 was 5 days before 2018-2023 mean, the range in isotherm date in 2019 was much larger, with some areas hitting the 0°C isotherm as much as 20 days before the 6-year mean. These observations broadly agree with anomalous conditions observed in 2019 throughout Alaska, as well as the Arctic more broadly. This year marked the second lowest winter sea ice extent in the Bering Sea since records began, which contributed to record-breaking warm ocean temperatures (Richter-Menge, 2019). Additionally, the overall sea ice extent for 2019 hit a historic low (since 1979), and the average annual land surface temperature north of 60° N was the second warmest since 1900 (Richter-Menge, 2019). Further, it was found to be the second highest decline in sea ice recorded (Yadav et. al, 2020). On a more local scale, a recent study within the same region (Yukon-Kuskokwim Delta) found that 2019 also had highly anomalously low landfast ice extent and earlier breakup timing (Cooley & Ryan, 2024). These similarities between the anomalous lake ice breakup in 2019 and other climate records thus emphasize connections between lake ice and other Arctic climate and cryosphere characteristics.

The anomalous characteristics observed in 2019 also serve as an illustration of the effects that increasing air temperatures may have on Arctic lake ice dynamics. If we presume that the conditions in 2019 may be indicative of future climate scenarios under continued global warming, we would expect not only earlier breakup occurrence but also increased spatial variability in breakup dates and a longer breakup season. This increased variability and longer breakup season length not only complicates predictions of breakup timing in the future but also amplifies the challenges faced by Arctic ecosystems and communities dependent on the stability and predictability of inland ice. Understanding and adapting to these shifts will thus be crucial in mitigating the impacts of climate change in Arctic regions.

5.5 | *Future Work*

The exploratory nature of this work meant that it was limited in scope, particularly regarding factors beyond temperature. Based on our findings that small lakes break up sooner and have a shorter lag interval, future work should investigate factors such as connectivity, morphometry, and precipitation in small lake environments. This will help determine if and how small lakes behave differently than large lakes. Additionally, investigating permafrost conditions, subsurface and surface water connectivity, and the proximity to major rivers and oceans could provide valuable context to the patterns observed in this study. Additionally, since small lakes consistently exhibit a wider interquartile range (IQR) of breakup dates compared to large lakes, further research is warranted. This variability suggests there are nuances in the ice breakup processes of small lakes that were not fully explored in this study. Future work should utilize Synthetic Aperture Radar (SAR) for detecting bedfast ice (Engram et al., 2018; Antonova et al., 2016) and examine the unique interactions and phenologies of small water bodies. Such research could uncover valuable details about the differences between bedfast and floating ice, providing a deeper understanding of the factors influencing ice breakup in small lakes. This is crucial for a comprehensive understanding of lake ice dynamics, particularly given the significant role small lakes play in regional hydrology and climate systems.

Our study area contains multiple communities who rely on lake ice and have local knowledge of its short- and long-term fluctuations. In this study, we did not have the opportunity or resources to work with such communities. However, we want to note that combining Western scientific findings with Indigenous knowledge would likely offer a more comprehensive approach to understanding changes in ice timing and quality. Indigenous observations provide essential on-the-ground information that is often missing from studies utilizing satellite-derived data. Engaging local communities in research from its inception enhances contextual understanding and improves the practical application of findings, creating potential for aiding in planning and increasing safety in the area (Herman-Mercer et al., 2011). Future work should make every effort to engage with local communities when appropriate and prioritize local questions; this is especially true in satellite-based research, which has a history of being extractive and/or out of context (Bennett, et. al, 2022).

6.0 | Conclusions

The annual formation and breakup of lake ice plays a crucial role in the hydrology, ecology, and socio-economic activities of Arctic regions. This study aimed to utilize Sentinel-2 optical imagery to investigate lake ice breakup dynamics in the Lower Kuskokwim River Watershed (LKRB) in Alaska, focusing on a large dataset of 145,955 lakes over a six-year period. Our findings demonstrate that Sentinel-2 imagery is effective for estimating ice breakup dates, with an average precision within 2.8 days of manually detected dates. The novel dataset created from this analysis offers valuable insights into the ice breakup patterns of both large and small lakes, filling a significant gap in our understanding of lake ice phenology in complex wetland environments.

Across our 6 year study period, we find that interannual variability generally exceeds spatial variability in breakup timing and that temperature (which also varies more interannually than spatially) is dominant driver of breakup patterns across varied lake sizes. We identify a consistent pattern of smaller lakes breaking up earlier than larger, which aligns with the hypothesis that smaller lakes, due to their lower heat capacity, respond more rapidly to temperature changes. Similarly, our results reveal smaller lakes break up sooner after the 0°C isotherm, indicating a faster thermal response to climatic conditions. These findings highlight the importance of including small lakes in climate models to improve their predictive capabilities and enhance our understanding of regional and local climatic conditions. Future work should explore previously studied factors (connectivity, morphometry, temperature) on small lake environments to better understand if and how small lakes behave differently than large lakes.

Appendix

Table 0: QA/QC results for ~175 randomly selected lakes between manually detected breakup date (via available satellite imagery) and novel Sentinel-2 methodology detected breakup. Performance indicates the number of days 'off' one estimate is from the other.

Lake ID	Manually Observed Breakup	Sentinel-2 Estimated Breakup	Performance (Days Off)
813	5/14/2022	5/12/2022	2.00
854	5/15/2022	5/14/2022	1.00
1607	5/7/2022	5/9/2022	2.00
1831	5/7/2022	5/9/2022	2.00
1874	5/7/2022	5/9/2022	2.00
2131	4/29/2022	5/13/2022	14.00
3525	5/11/2022	5/13/2022	2.00
3923	4/29/2022	5/1/2022	2.00
4763	5/8/2022	5/13/2022	5.00
6739	4/29/2022	5/1/2022	2.00
7263	5/20/2022	5/21/2022	1.00
7347	5/5/2022	5/4/2022	1.00
7863	5/9/2022	5/18/2022	9.00
8124	5/7/2022	5/13/2022	6.00
8802	5/18/2022	5/18/2022	0.00
9211	5/9/2022	5/11/2022	2.00
9705	5/18/2022	5/18/2022	0.00
10605	5/20/2022	5/21/2022	1.00
11277	5/11/2022	5/12/2022	1.00
11287	5/3/2022	5/13/2022	10.00
11707	5/15/2022	5/13/2022	2.00
12031	4/29/2022	5/2/2022	3.00
13551	5/11/2022	5/13/2022	2.00
13758	5/11/2022	5/12/2022	1.00
14614	5/15/2022	5/14/2022	1.00
14743	5/16/2022	5/16/2022	0.00
14759	5/11/2022	5/13/2022	2.00
16389	5/18/2022	5/18/2022	0.00
16557	5/9/2022	5/13/2022	4.00
17630	5/9/2022	5/13/2022	4.00
17764	5/13/2022	5/13/2022	0.00
18330	5/9/2022	5/13/2022	4.00
18368	5/11/2022	5/13/2022	2.00
18416	5/12/2022	5/13/2022	1.00
18909	5/15/2022	5/16/2022	1.00
20882	5/9/2022	5/11/2022	2.00
21107	5/12/2022	5/11/2022	1.00
21679	5/16/2022	5/17/2022	1.00
23944	5/16/2022	5/16/2022	0.00
25321	5/3/2022	5/12/2022	9.00
27147	5/7/2022	5/12/2022	5.00
28941	5/10/2022	5/13/2022	3.00
29663	4/29/2022	4/30/2022	1.00
29687	5/15/2022	5/14/2022	1.00
29958	5/7/2022	5/3/2022	4.00
31535	5/9/2022	5/12/2022	3.00
32527	5/12/2022	5/12/2022	0.00
33252	4/29/2022	4/30/2022	1.00
33804	4/29/2022	4/30/2022	1.00
34109	5/17/2022	5/16/2022	1.00
34546	5/9/2022	5/12/2022	3.00
34586	5/9/2022	5/12/2022	3.00
35295	5/9/2022	5/12/2022	3.00
38430	4/30/2022	4/29/2022	1.00
39087	5/9/2022	5/12/2022	3.00
40307	5/12/2022	5/12/2022	0.00
42106	5/9/2022	4/30/2022	9.00
42300	4/29/2022	4/28/2022	1.00
43516	5/2/2022	5/2/2022	0.00
44386	5/9/2022	5/12/2022	3.00
44600	5/15/2022	5/14/2022	1.00
46784	5/6/2022	5/4/2022	2.00
49012	4/29/2022	4/30/2022	1.00
49552	5/12/2022	5/13/2022	1.00
49893	4/30/2022	5/1/2022	1.00
50128	5/9/2022	5/12/2022	3.00
51092	5/12/2022	5/11/2022	1.00
51445	5/7/2022	5/11/2022	4.00
53800	5/12/2022	5/13/2022	1.00
54442	5/15/2022	5/14/2022	1.00
54721	5/12/2022	5/12/2022	0.00
55777	5/7/2022	5/13/2022	6.00
57094	5/7/2022	5/9/2022	2.00
57810	5/11/2022	5/11/2022	0.00
58349	5/11/2022	5/13/2022	2.00

58428	5/15/2022	5/15/2022	0.00
59135	5/5/2022	5/12/2022	7.00
60470	5/7/2022	5/17/2022	10.00
60626	5/10/2022	5/18/2022	8.00
60746	5/15/2022	5/16/2022	1.00
60818	5/18/2022	5/18/2022	0.00
61029	5/15/2022	5/15/2022	0.00
62356	5/12/2022	5/11/2022	1.00
62860	4/23/2022	5/12/2022	19.00
63411	5/1/2022	4/30/2022	1.00
63623	5/18/2022	5/1/2022	17.00
63726	5/11/2022	5/13/2022	2.00
63870	5/10/2022	5/12/2022	2.00
64144	5/19/2022	5/17/2022	2.00
66376	5/15/2022	5/13/2022	2.00
68209	5/16/2022	5/16/2022	0.00
68716	5/15/2022	5/15/2022	0.00
69483	5/23/2022	5/22/2022	1.00
70452	5/7/2022	5/11/2022	4.00
71238	5/19/2022	5/17/2022	2.00
72082	5/15/2022	5/15/2022	0.00
72220	4/29/2022	5/3/2022	4.00
72240	5/9/2022	5/12/2022	3.00
72919	5/7/2022	5/12/2022	5.00
72950	5/2/2022	5/1/2022	1.00
73395	5/1/2022	5/1/2022	0.00
74062	5/15/2022	5/13/2022	2.00
74473	5/13/2022	5/7/2022	6.00
74791	5/18/2022	5/17/2022	1.00
74835	5/19/2022	5/20/2022	1.00
76528	4/29/2022	4/30/2022	1.00
76938	5/6/2022	5/13/2022	7.00
77277	5/11/2022	5/13/2022	2.00
77590	5/4/2022	5/11/2022	7.00
78229	5/13/2022	5/13/2022	0.00
80207	5/2/2022	5/1/2022	1.00
81216	4/29/2022	4/29/2022	0.00
81423	5/7/2022	5/5/2022	2.00
81562	5/3/2022	5/3/2022	0.00
86256	4/28/2022	4/1/2022	27.00
89428	5/9/2022	5/12/2022	3.00
90014	5/9/2022	5/12/2022	3.00
90203	5/9/2022	5/12/2022	3.00
90239	5/8/2022	5/12/2022	4.00

90840	5/7/2022	5/12/2022	5.00
91831	4/28/2022	4/29/2022	1.00
93029	5/2/2022	4/30/2022	2.00
93916	5/7/2022	5/11/2022	4.00
94599	4/29/2022	4/30/2022	1.00
95181	4/29/2022	4/30/2022	1.00
95248	5/15/2022	5/11/2022	4.00
96316	4/4/2022	5/4/2022	30.00
96664	5/14/2022	5/12/2022	2.00
96860	5/11/2022	5/11/2022	0.00
97386	5/2/2022	5/3/2022	1.00
97620	5/5/2022	5/2/2022	3.00
98339	5/3/2022	5/3/2022	0.00
99707	5/3/2022	5/2/2022	1.00
101541	5/7/2022	5/1/2022	6.00
103534	5/7/2022	5/1/2022	6.00
105747	5/9/2022	5/13/2022	4.00
105784	5/20/2022	5/19/2022	1.00
106231	5/15/2022	5/16/2022	1.00
107463	5/21/2022	5/21/2022	0.00
109705	5/18/2022	5/17/2022	1.00
111177	5/11/2022	5/13/2022	2.00
111362	5/3/2022	5/13/2022	10.00
111376	4/29/2022	4/30/2022	1.00
111379	5/17/2022	5/16/2022	1.00
112573	5/18/2022	5/16/2022	2.00
112645	5/9/2022	5/13/2022	4.00
115816	5/12/2022	5/13/2022	1.00
117115	5/13/2022	5/13/2022	0.00
118501	5/7/2022	5/15/2022	8.00
120865	4/29/2022	5/3/2022	4.00
122237	5/12/2022	5/12/2022	0.00
123020	5/2/2022	4/30/2022	2.00
129030	5/18/2022	5/17/2022	1.00
129273	5/9/2022	5/5/2022	4.00
129899	5/20/2022	5/20/2022	0.00
130637	5/14/2022	5/12/2022	2.00
130679	5/20/2022	5/25/2022	5.00
130887	5/15/2022	5/14/2022	1.00
131882	5/18/2022	5/17/2022	1.00
136690	5/7/2022	5/12/2022	5.00
137227	5/9/2022	5/12/2022	3.00
137693	5/9/2022	5/12/2022	3.00
137811	5/12/2022	5/11/2022	1.00

138709	5/14/2022	5/13/2022	1.00
139442	5/18/2022	5/16/2022	2.00
139451	5/18/2022	5/17/2022	1.00
139533	5/20/2022	5/20/2022	0.00
139601	5/15/2022	5/15/2022	0.00
140243	5/19/2022	5/18/2022	1.00
141001	5/6/2022	5/3/2022	3.00
143242	5/11/2022	5/11/2022	0.00
143908	4/29/2022	5/3/2022	4.00
144043	5/7/2022	5/9/2022	2.00
144787	5/9/2022	5/14/2022	5.00
145927	5/3/2022	5/4/2022	1.00
147937	4/29/2022	5/1/2022	2.00
148598	4/29/2022	5/1/2022	2.00

Table 1: Breakup date (DOY) and associated uncertainty summary (± X days) statistics (corresponding to Figure 3)

	Breakup					
Year	**Mean**	**Med.**	**SD**	**Q1**	**Q3**	**IQR**
2018	136.22	136	9.21	131	141	10
2019	126.16	123	12.29	119	132	13
2020	128.00	127	8.70	124	133	9
2021	137.40	139	7.67	133	142	9
2022	128.77	132	8.16	121	134	13
2023	147.50	147	11.70	138	156	18

	Uncertainty							
Year	**Min**	**Max.**	**Mean**	**Med.**	**SD**	**IQR**	**% lakes ± 2 days**	**% lakes ± 5 days**
2018	0.5	32.5	9.290	7.5	7.28	11.5	15.22	41.27
2019	0.5	29	4.306	3.5	3.86	2.5	26.19	81.69
2020	0.5	22.5	2.442	2.5	1.98	1.5	48.91	93.57
2021	0.5	21.5	6.366	6	3.58	6.5	14.63	45.96
2022	0.5	6.5	2.149	1.5	1.26	1.5	52.62	99.79
2023	0.5	13.5	4.630	4.5	2.98	4	28.98	65.54

Table 2: Breakup Date (DOY) and associated uncertainty (± X days) summary statistics by size group (corresponding to Figure 5)

			Breakup				
Year	**Size**	**Min.**	**Max.**	**Mean**	**Med.**	**SD**	**IQR**
2018	Large	92	179	141.28	140	8.30	10.25
2018	Small	92	179	136.20	136	9.22	10
2019	Large	96	175	133.68	132	10.56	11
2019	Small	92	179	126.13	123	12.29	13
2020	Large	111	163	134.82	134	8.02	7
2020	Small	97	180	127.97	127	8.69	9
2021	Large	102	171	140.54	142	5.87	5

2021	Small	99	175	137.39	139	7.68	9
2022	Large	100	165	136.21	137	6.54	7
2022	Small	102	178	128.73	132	8.16	13
2023	Large	96	179	151.85	152	9.78	11
2023	Small	94	179	147.48	147	11.71	18

				Uncertainty				
Year	**Size**	**Min.**	**Max.**	**Mean**	**Med.**	**SD**	**IQR**	**Count**
2018	Large	0.5	32.5	8.80	6	7.77	11.5	800
2018	Small	0.5	32.5	9.29	7.5	7.28	11.5	145011
2019	Large	0.5	22.5	5.48	4	3.99	4	789
2019	Small	0.5	29	4.30	3.5	3.86	2.5	145012
2020	Large	0.5	21	3.03	2.5	2.53	2	797
2020	Small	0.5	22.5	2.44	2.5	1.98	1.5	145040
2021	Large	0.5	17.5	6.33	6	3.58	6.5	799
2021	Small	0.5	21.5	6.37	6	3.58	6.5	145152
2022	Large	0.5	5.5	1.70	1.5	1.02	0.5	785
2022	Small	0.5	6.5	2.15	2	1.26	1.5	144861
2023	Large	0.5	13.5	4.54	5	2.95	4	778
2023	Small	0.5	13.5	4.63	4.5	2.98	4	144660

Table 3: Yearly 0°C isotherm date (DOY) summary statistics (corresponding to Figure 6)

Year	***Mean***	***Med.***	***SD***	***Min.***	***Max.***	***IQR***
2018	121.7262	122	3.337939	113	145	5
2019	120.8425	125	13.1037	51	142	20
2020	122.9637	122	3.185129	115	132	4
2021	127.871	128	0.906341	125	135	1
2022	121.9687	122	3.668923	115	143	5
2023	137.7503	138	1.254097	135	150	1

Table 4: Yearly correlation for relationship between 0°C Isotherm (corresponding to Figure 7)

Year	***R^2***	***P Value***
2018	0.000428	2.96E-15
2019	0.308299	0
2020	0.097284	0
2021	0.328071	0
2022	0.09344	0
2023	0.065598	0
All Years	0.311095	0

Table 5: Yearly lag interval summary statistics (corresponding to Figure 8)

Year	Min.	Max.	Mean	Med.	SD	IQR
2018	-35	62	14.51516	13	9.734849	13
2019	-41	96	5.305053	2	11.99033	15
2020	-26	57	5.010175	5	8.284086	9
2021	-29	46	8.847601	10	7.164621	8
2022	-28	57	6.902601	9	7.975815	11
2023	-48	41	9.795289	10	11.54773	16

Table 6: Yearly lag interval summary statistics by size group (corresponding to Figure 9)

Year	Lake Size	Min.	Max.	Mean	Med.	SD	IQR
2018	Large	-27	47	19.92139	20	8.459711	12
2018	Small	-35	62	14.48614	13	9.733169	13
2019	Large	-26	65	11.50828	10	11.4481	13
2019	Small	-41	96	5.271427	2	11.9845	15
2020	Large	-13	42	11.92714	11	8.1557	9
2020	Small	-26	57	4.971905	5	8.268739	9
2021	Large	-26	40	12.30374	14	5.798457	5
2021	Small	-29	46	8.671567	10	7.257265	8
2022	Large	-21	33	14.75152	16	6.911894	8
2022	Small	-28	57	6.860164	9	7.960199	11
2023	Large	-32	40	14.45611	14.5	9.246686	11
2023	Small	-48	41	9.770744	10	11.55369	16

Table 7: Summary statistics of error between Sentinel-2 estimated breakup date and lag interval estimated breakup date (corresponding to Figure 11b). Additionally broken up by size for comparison between size groups.

Lake Size	Mean	Median	SD	Max.
Large	5.768471	4.666667	4.720732	39.33333
Small	6.821086	5.4	5.716695	74
All Lakes	6.815419	5.4	5.712316	74

REFERENCES CITED

Arp, C. D., & Jones, B. M. (2009). Geography of Alaska Lake Districts: Identification, Description, and Analysis of Lake-Rich Regions of a Diverse and Dynamic State. *USGS Scientific Investigations Report*. https://pubs.usgs.gov/sir/2008/5215/

Arp, C. D., Jones, B. M., & Grosse, G. (2013). Recent lake ice-out phenology within and among lake districts of Alaska, U.S.A. *Limnology and Oceanography*, *58*(6), 2013–2028. https://doi.org/10.4319/lo.2013.58.6.2013

Arp, C. D., Jones, B. M., Liljedahl, A. K., Hinkel, K. M., & Welker, J. A. (2015). Depth, ice thickness, and ice-out timing cause divergent hydrologic responses among Arctic lakes, *Water Resour. Res*., 51, 9379–9401, doi:10.1002/2015WR017362.

Antonova, S., Duguay, C. R., Kääb, A., Heim, B., Langer, M., Westermann, S., & Boike, J. (2016). Monitoring Bedfast Ice and Ice Phenology in Lakes of the Lena River Delta Using TerraSAR-X Backscatter and Coherence Time Series. Remote Sensing, 8(11), Article 11. https://doi.org/10.3390/rs8110903

Assel, R., & Robertson, D. (1995). Changes in winter air temperatures near Lake-Michigan, 1851–1993, as determined from regional lake-ice records. *Limnol. Oceanogr. 40: 165–176*, doi:10.4319/lo.1995.40.1.0165

Austin, J. A., & Colman, S. M. (2007). Lake Superior summer water temperatures are increasing more rapidly than regional air temperatures: A positive ice-albedo feedback. *Geophys. Res. Lett., 34*, L06604, doi:10.1029/2006GL029021.

Barbieux, K., Charitsi, A., & Merminod, B. (2018). Icy lakes extraction and water-ice classification using Landsat 8 OLI multispectral data. *International Journal of Remote Sensing,* 39(11), 3646–3678. https://doi.org/10.1080/01431161.2018.1447165

Benke, A. C., & Cushing, C. E. (2011). *Rivers of North America*. Elsevier.

Bennett, M. M., Chen, J. K., Alvarez León, L. F., & Gleason, C. J. (2022). The politics of pixels: A review and agenda for critical remote sensing. Progress in Human Geography, 46(3), 729–752. https://doi.org/10.1177/03091325221074691

Benson, B., J. Magnuson, and S. Sharma. (2000). Global Lake and River Ice Phenology Database, Version 1. Boulder, Colorado USA. National Snow and Ice Data Center. https://doi.org/10.7265/N5W66HP8.

Bring, A., Fedorova, I., Dibike, Y., Hinzman, L., Mård, J., Mernild, S. H., Prowse, T., Semenova, O., Stuefer, S. L., & Woo, M.-K. (2016). Arctic terrestrial hydrology: A synthesis of processes, regional effects, and research challenges. *Journal of Geophysical Research: Biogeosciences*, *121*(3), 621–649. https://doi.org/10.1002/2015JG003131

Brown, L., & Duguay, C. (2010). The response and role of ice cover in lake-climate interactions. *Progress in Physical Geography*, *34*, 671–704. https://doi.org/10.1177/0309133310375653

Cooley, S. W., Ryan, J. C., Smith, L. C., Horvat, C., Pearson, B., Dale, B., & Lynch, A. H. (2020). Coldest Canadian Arctic communities face greatest reductions in shorefast sea ice. *Nature Climate Change, 10(6)*, 533–538. https://doi.org/10.1038/s41558-020-0757-5

Cooley, S. W., & Ryan, J. C. (2024). Community-scale changes to landfast ice along the coast of Alaska over 2000-2022. *Environmental Research Letters*, *19*(2), 024013. https://doi.org/10.1088/1748-9326/ad1c7b

Cory, R.M., Ward, C.P., Crump, B.C., & Kling, G.W. (2014). Carbon cycle. Sunlight controls water column processing of carbon in arctic fresh waters. *Science, 22;345(6199)*:925-8. doi: 10.1126/science.1253119. PMID: 25146289.

Dibike, Y., Prowse, T., Saloranta, T., & Ahmed, R. (2011). Response of Northern Hemisphere lake-ice cover and lake-water thermal structure patterns to a changing climate. *Hydrological Processes*, *25*, 2942–2953. https://doi.org/10.1002/hyp.8068

Dolan, W., Pavelsky, T. M., & Yang, X. (2021). Functional Lake-to-Channel Connectivity Impacts Lake Ice in the Colville Delta, Alaska. *Journal of Geophysical Research: Earth Surface*, *126*(12), e2021JF006362. https://doi.org/10.1029/2021JF006362

Downing, J. A., Prairie, Y. T., Cole, J. J., Duarte, C. M., Tranvik, L. J., Striegl, R. G., McDowell, W. H., Kortelainen, P., Caraco, N. F., Melack, J. M., & Middelburg, J. J. (2006). The global abundance and size distribution of lakes, ponds, and impoundments. *Limnol. Oceanogr. 51: 2388–2397*, doi:10.4319/lo.2006.51.5.2388

Duguay, C.R., Flato, G.M., Jeffries, M.O., Ménard, P., Morris, K. & Rouse, W.R. (2003). Ice-cover variability on shallow lakes at high latitudes: model simulations and observations. *Hydrol. Process., 17:* 3465-3483. https://doi.org/10.1002/hyp.1394

Engram, M., Arp, C. D., Jones, B. M., Ajadi, O. A., & Meyer, F. J. (2018). Analyzing floating and bedfast lake ice regimes across Arctic Alaska using 25 years of space-borne SAR imagery. Remote Sensing of Environment, 209, 660–676. https://doi.org/10.1016/j.rse.2018.02.022

Futter, M. (2003). Patterns and trends in Southern Ontario lake ice phenology. *Environ. Monit. Assess.* 88: 431–444, doi:10.1023/A:1025549913965

Graham, R. M., Hudson, S. R., & Maturilli, M. (2019). Improved Performance of ERA5 in Arctic Gateway Relative to Four Global Atmospheric Reanalyses. *Geophysical Research Letters*, 46(11), 6138–6147. https://doi.org/10.1029/2019GL082781

Herman-Mercer, N., Schuster, P., & Maracle, K. (2011). Indigenous Observations of Climate Change in the Lower Yukon River Basin, Alaska. *Human Organization*, *70*, 244–252. https://doi.org/10.17730/humo.70.3.v88841235897071m

Herman-Mercer, N. M., Laituri, M., Massey, M., Matkin, E., Toohey, R. C., Elder, K., Schuster, P. F., & Mutter, E. (2019). Vulnerability of Subsistence Systems Due to Social and Environmental Change: A Case Study in the Yukon-Kuskokwim Delta, Alaska. *Arctic*, 72(3), 258–272. https://www.jstor.org/stable/26822411

Holgerson, M. A., & Raymond, P. A. (2016). Large contribution to inland water CO2 and CH4 emissions from very small ponds. *Nature Geoscience*, 9(3), 222–226. https://doi.org/10.1038/ngeo2654

Ingram, W. J., Wilson, C. A., & Mitchell, J. F. B. (1989). Modeling climate change: An assessment of sea ice and surface albedo feedbacks, *J. Geophys. Res., 94(D6*), 8609–8622, doi:10.1029/JD094iD06p08609.

Instanes, A., Kokorev, V., Janowicz, R., Bruland, O., Sand, K., & Prowse, T. (2016). Changes to freshwater systems affecting Arctic infrastructure and natural resources. *Journal of Geophysical Research: Biogeosciences*, *121*(3), 567–585. https://doi.org/10.1002/2015JG003125

Jeffries, Martin & Morris, Kim. (2007). Some aspects of ice phenology on ponds in central Alaska, USA. *Annals of Glaciology* - ANN GLACIOL. 46. 10.3189/172756407782871576.

Korhonen, Johanna. (2006). Long-term changes in lake ice cover in Finland. *Water Policy*. 37. 10.2166/nh.2006.019.

Lang, J., Lyu, S., Li, Z., Ma, Y., & Su, D. (2018). An Investigation of Ice Surface Albedo and Its Influence on the High-Altitude Lakes of the Tibetan Plateau. *Remote Sens., 10, 218*. https://doi.org/10.3390/rs10020218

Lesi, M., Nie, Y., Shugar, D. H., Wang, J., Deng, Q., Chen, H., & Fan, J. (2022). Landsat- and Sentinel-derived glacial lake dataset in the China–Pakistan Economic Corridor from 1990 to 2020. *Earth System Science Data*, 14(12), 5489–5512. https://doi.org/10.5194/essd-14-5489-2022

Liu, C., Huang, H., Hui, F., Zhang, Z., & Cheng, X. (2021). Fine-Resolution Mapping of Pan-Arctic Lake Ice-Off Phenology Based on Dense Sentinel-2 Time Series Data. *Remote Sensing*, 13(14), Article 14. https://doi.org/10.3390/rs13142742

Levenson, E.S., Cooley, S.W., Mullen, A.L., Webb, E., Watts., J.D. (in prep). Constraining permafrost controls on the distribution of lakes and ponds across Alaska using a new high-resolution lake dataset.

Muñoz Sabater, J. (2019): ERA5-Land hourly data from 1950 to present. Copernicus Climate Change Service (C3S) Climate Data Store (CDS). DOI: 10.24381/cds.e2161bac

Obu, J., Westermann, S., Bartsch, A., Berdnikov, N., Christiansen, H. H., Dashtseren, A., Delaloye, R., Elberling, B., Etzelmüller, B., Kholodov, A., Khomutov, A., Kääb, A., Leibman, M. O., Lewkowicz, A. G., Panda, S. K., Romanovsky, V., Way, R. G., Westergaard-Nielsen, A., Wu, T., … Zou, D. (2019). Northern Hemisphere permafrost map based on TTOP modelling for 2000–2016 at 1 km2 scale. *Earth-Science Reviews*, *193*, 299–316. https://doi.org/10.1016/j.earscirev.2019.04.023

Pavelsky, T. M., & Smith, L. C. (2004). Spatial and temporal patterns in Arctic river ice breakup observed with MODIS and AVHRR time series. *Remote Sensing of Environment*, 93(3), 328–338. https://doi.org/10.1016/j.rse.2004.07.018

Prowse, T. D., Bonsal, B. R., Duguay, C. R., & Lacroix, M. P. (2007). River-ice break-up/freeze-up: a review of climatic drivers, historical trends and future predictions. *Annals of Glaciology*, *46, 443–451*. doi:10.3189/172756407782871431

Prowse, T., Alfredsen, K., Beltaos, S. et al. (2011c). Arctic freshwater ice and its climatic role. *Ambio 40: 46–52*, doi:10.1007/s13280-011-0214-9

Richter-Menge, J., Druckenmiller, M. L., & Jeffries, M. (2019). *Arctic Report Card 2019*, https://www.arctic.noaa.gov/Report-Card.

Robertson, D., Ragotzkie, R., & Magnuson, J. (1992). Lake ice records used to detect historical and future climatic changes. *Clim. Change 21*: 407–427, doi:10.1007/BF00141379

Schindler, D.W., Beaty, K., & Turner, M. (1990). Effects of climatic warming on lakes of the central boreal forest. *Science 250*: 967–970, doi:10.1126/science.250.4983.967

Seaber, P., Kapinos, P., & Knapp, G. (1987). Hydrologic Unit Maps. *USGS Water-Supply Paper 2294*.

Sharma, S., Filazzola, A., Nguyen, T., Imrit, M. A., Blagrave, K., Bouffard, D., Daly, J., Feldman, H., Feldsine, N., Hendricks-Franssen, H.-J., Granin, N., Hecock, R., L'Abée-

Lund, J. H., Hopkins, E., Howk, N., Iacono, M., Knoll, L. B., Korhonen, J., Malmquist, H. J., … Magnuson, J. J. (2022). Long-term ice phenology records spanning up to 578 years for 78 lakes around the Northern Hemisphere. *Scientific Data, 9(1),* 318. https://doi.org/10.1038/s41597-022-01391-6

Šmejkalová, T., Edwards, M. E., & Dash, J. (2016). Arctic lakes show strong decadal trend in earlier spring ice-out. *Scientific Reports*, *6*(1), 38449. https://doi.org/10.1038/srep38449

Smol, J. P., & Douglas, M. S. V. (2007). Crossing the final ecological threshold in high Arctic ponds. *Proceedings of the National Academy of Sciences*, 104(30), 12395–12397. https://doi.org/10.1073/pnas.0702777104

Swart, N. C., Fyfe, J. C., Hawkins, E., Kay, J. E., & Jahn, A. (2015). Influence of internal variability on Arctic sea-ice trends. *Nature Climate Change*, 5, 86-89. doi:10.1038/nclimate2483

Tuttle, S.E., Roof, S.R., Retelle, M.J., Werner, A., Gunn, G.E., & Bunting, E.L. (2022). Evaluation of Satellite-Derived Estimates of Lake Ice Cover Timing on Linnévatnet, Kapp Linné, Svalbard Using In-Situ Data. *Remote Sens. 14,* 1311. https://doi.org/10.3390/rs14061311

U.S. Census Bureau. (2020). *Bethel city, Alaska*. Retrieved [May, 2024], from https://data.census.gov/profile/Bethel_city,_Alaska?g=160XX00US0206520#populations-and-people.

Vihma, T., Screen, J., Tjernström, M., Newton, B., Zhang, X., Popova, V., Deser, C., Holland, M., & Prowse, T. (2016). The atmospheric role in the Arctic water cycle: A review on processes, past and future changes, and their impacts. *Journal of Geophysical Research: Biogeosciences*, *121*(3), 586–620. https://doi.org/10.1002/2015JG003132

Vincent, A. C., Mueller, D. R., & Vincent, W.F. (2008). Simulated heat storage in a perennially ice-covered high Arctic lake: Sensitivity to climate change, J. Geophys. Res., 113, C04036, doi:10.1029/2007JC004360.

Wang, J., Sheng, Y., Hinkel, K.M., & Lyons, E. (2016). Alaskan Lake Database Mapped from Landsat Images. Arctic Data Center. doi:10.5065/D6MC8X5R.

Walter, K., Chanton, J., Chapin III, F., Schuur, E., & Zimov, S. (2008). Methane production and bubble emissions from arctic lakes: Isotopic implications for source pathways and ages, *J. Geophys. Res.*, 113, G00A08, doi:10.1029/2007JG000569.

Weyhenmeyer, G. A., Meili, M., & Livingstone, D. M. (2004). Nonlinear temperature response of lake ice breakup. *Geophysical Research Letters*, *31*(7). https://doi.org/10.1029/2004GL019530

Wik, M., Varner, R., Walter Anthony, K., Macintyre, S., & Bastviken, D. (2016). Climate-sensitive northern lakes and ponds are critical components of methane release. *Nature Geoscience*, *9*. https://doi.org/10.1038/ngeo2578

Williams, S.G., & Stefan, H.G. (2006). Modeling of lake ice characteristics in North America using climate, geography, and lake bathymetry. *Journal of Cold Regions Engineering 20: 140–167.* https://doi.org/10.1061/(ASCE)0887-381X(2006)20:4(140)

Wrona, F. J., Johansson, M., Culp, J. M., Jenkins, A., Mård, J., Myers-Smith, I. H., Prowse, T. D., Vincent, W. F., & Wookey, P. A. (2016). Transitions in Arctic ecosystems: Ecological implications of a changing hydrological regime. *Journal of Geophysical Research: Biogeosciences*, *121*(3), 650–674. https://doi.org/10.1002/2015JG003133

Zhang, S., & Pavelsky, T. M. (2019). Remote Sensing of Lake Ice Phenology across a Range of Lakes Sizes, ME, USA. *Remote Sensing*, *11*(14), Article 14. https://doi.org/10.3390/rs11141718

Zhang, S., Pavelsky, T. M., Arp, C. D., & Yang, X. (2021). Remote sensing of lake ice phenology in Alaska. *Environmental Research Letters*, *16*(6), 064007. https://doi.org/10.1088/1748-9326/abf965

Zhang, Y., Fregona, M., Loehr, J., Ala-Könni, J., Song, S., Leppäranta, M., & Li, Z. (2023). A field study on ice melting and breakup in a boreal lake, Pääjärvi, in Finland. *The Cryosphere*, *17(5),* 2045–2058. https://doi.org/10.5194/tc-17-2045-2023.